TARGETING PROTEIN INTERACTIONS OF FAK AND IGF-1R IN HUMAN CANCER AS A NOVEL ANTI-NEOPLASTIC APPROACH

By

DENIZ A. UCAR

A DISSERTATION PRESENTED TO THE GRADUATE SCHOOL
OF THE UNIVERSITY OF FLORIDA IN PARTIAL FULFILLMENT
OF THE REQUIREMENTS FOR THE DEGREE OF
DOCTOR OF PHILOSOPHY

UNIVERSITY OF FLORIDA

2010

To my loves Mine and Arslan Ucar

ACKNOWLEDGMENTS

From the bottom of my heart, I would first like to thank my mentor, Dr. Steven N. Hochwald who provided me the opportunity to work on this project, endured and patiently supported my endless demands. I gratefully thank Dr. Elena Kurenova for her excellent guidance and opportunities she has provided me during my stay in this lab. I would also thank Dr. William Cance who provided the support for this project. I would also like to thank my committee members, Drs. Thomas Rowe, Brian Law, and James Resnic, for their time, positive energy, and guidance. I would also appreciate the members of the "Cance/Hochwald lab," especially DiHua He, Carl Nyberg, Donghan Zheng, and Audrey Cox. My deepest thanks also are extended to my friends Marda Jorgensen for her invaluable guidance and time for immunohistochemistry analysis; Steve McClellan for his time, patience and efforts to help me for FACS analysis and confocal imaging. I also gratefully thank Dr. Lung-Ji Chang for his guidance and support for the transfection of cells. I would like to thank Dr. Wayne McCormack for his endless support and motivation though out my Master's and PhD programs. Their help was invaluable and their presence made work a pleasant place.

I also appreciate Joyce Conners for her endless support since the day I met her six years ago. She has been a wonderful caring 'American Mom.' I would also include my previous professors; Dr. Philip Laipis, Dr. Edward Scott and their lab members in my list of the people who I deeply appreciate for their guidance and continuing friendships. I thank also flow cytometry core members, especially Neal Benson for giving me technical advice on many occasions and for their help in maintain the core.

Outside the UF, and most importantly, I would like to thank my parents, Mine and Arslan Ucar, my sister, Derya Sehri and her family, my brother, Yigit Ucar and his family. Although they live in Turkey, whenever I need them, they do not hesitate to travel a thousand miles to be

beside me. I do appreciate them for their support and caring. I would like to thank my friends, Robert Fisher, Shuhong Han, Qing Yang, Jennifer Stamp, Robert Mann, Brian Motyer, Jennifer Barrell, and Slava, who have provided strength, wisdom, motivation, and love. Finally, the biggest thanks is reserved for my doctor Bulent Urman, whose surgical skills and expertise provided me a cancer free life.

I DO LOVE ALL OF THEM.

TABLE OF CONTENTS

page

LIST OF TABLES

LIST OF FIGURES

Abstract of Dissertation Presented to the Graduate School
of the University of Florida in Partial Fulfillment of the
Requirements for the Degree of Doctor of Philosophy

TARGETING PROTEIN INTERACTIONS OF FAK AND IGF-1R IN HUMAN CANCER AS A NOVEL ANTI-NEOPLASTIC APPROACH

By

Deniz A. Ucar

May 2010

Chair: Steven N. Hochwald
Major: Medical Sciences - Genetics

Previously, we have shown that FAK (focal adhesion kinase) and IGF-1R (insulin-like growth factor receptor-1) directly interact with each other and this interaction provides activation of crucial signaling pathways that benefit cancer cells. Inhibition of FAK and IGF-1R function by knock down of genes and kinase inhibitors have shown to significantly decrease cancer cell proliferation and decrease resistance to chemotherapy and radiation treatment. In this study, as a novel approach, I evaluated the effect of a small molecule compound that disrupts the interaction of FAK and IGF-1R.

Using virtual screening and functional testing, I identified a lead compound INT2-31 that targets the known FAK-IGF-1R interaction site. I studied the effect of this compound on FAK-IGF-1R protein interactions, when administered alone or in combination with 5-FU or gemcitabine chemotherapy on cell signaling, viability and apoptosis in human melanoma (A375, C8161, SK-Mel28), esophageal (KYSE 70, 140) and pancreatic (Miapaca-2, Panc-1) cancer cells and on *in vivo* tumor growth in xenograft mouse models.

Based on GST pull down assay with purified protein fragments of FAK-FERM domain and IGF-1Rβ, I concluded that INT2-31 blocked the interaction of FAK and IGF-1R. INT2-31 caused a disruption of protein interactions between FAK and IGF-1R *in vitro* in cancer cells

starting at a concentration of 2.5 μM. It also caused a dose dependent inhibition of cell viability and induction of apoptosis starting at doses of 0.5 μM and 5μM, respectively. These effects were associated with a decrease in phosphorylation of Akt and ERK1/ERK2. Furthermore, treatment with INT2-31 sensitized cancer cells to chemotherapy since 5-FU synergistically decreased cell growth and increased apoptosis when combined with INT2-31 compared to 5-FU or INT2-31 alone.

In vivo INT2-31 treatment has dramatic inhibitory effect on tumor growth, when administered via subcutaneous or intraperitoneal injection, at 15 to 50mg/kg daily, in both subcutaneous xenografts and pancreatic orthotopic mouse models. For instance, the size of the tumor, grown from an esophageal cancer specimen in the subcutaneous location was reduced by 70% in INT2-31 treated animals vs control (236 $\pm$131 vs 931 $\pm$375 mm^3, respectively, $p<0.005$). This was associated with a decrease in cell proliferation (tumors from INT2-31 treated animals stained with Ki67 demonstrated a significant decrease in positive cells 52% vs 32%, control vs INT2-31, respectively, $p<0.05$) and decreased activation of p-AKT in tumor cells.

Our data suggest that the FAK-IGF-1R protein interaction is an important target and disruption of this protein-protein interaction with a small molecule has a potential anti-neoplastic therapeutic effect.

CHAPTER 1
INTRODUCTION AND BACKGROUND

Despite recent advances in conventional cancer treatment methods, survival of cancer patients remains suboptimal. Fortunately, the revolution in cancer research expanded our knowledge about mechanisms involved in tumor initiation and progression. Therefore, specific aberrancies in tumors and their microenvironment can be uncovered and targeted for the development of new anti-cancer drugs.

Growing evidence indicates that cancer cells progress through altered signaling pathways. Malignant cells acquire aberrations that favor their survival, growth, invasion and motility. Among these key regulatory factors, insulin like growth factor receptor (IGF-1R) and focal adhesion kinase (FAK) are tyrosine kinases which have been shown to be over expressed in many human cancers and play an important role in signal transduction of the malignant phenotype (Kanter-Lawensohn et al. 1998, Kanter-Lawensohn et al. 2000, Kahana et al. 2002, Mori et al. 1996, Liu et al. 2002, Ouban et al. 2003, Zheng et al. 2009, Liu et al. 2008). In addition, both of these proteins have shown to be involved in chemo and radiation resistance as well as inducing cell survival and proliferation. We previously identified the site of interaction between FAK and IGF-1R. We hypothesize that the FAK and IGF-1R interaction provides survival signals for cancer cells and disruption of this binding with novel small molecules can inhibit essential signaling pathways and inhibit tumor growth.

Focal Adhesion Kinase

Focal Adhesion Kinase (FAK) is a key regulatory factor of the cell signaling cascade initiated either at the site of cell attachment or at growth factor receptors. In normal cells, FAK and adhesion signaling pathways are involved in important and interesting cellular processes, including development, vascular function, and repair. On the other hand, activation of FAK plays

an important role in survival, proliferation, migration and invasion of cancer cells that are crucial in the development and progression of malignancies. In many cancers, there is a correlation between over expression of FAK and progression to higher-grade malignancy. In invasive and metastatic human breast and colon cancer, FAK expression has shown to be up regulated compared to normal tissue (Weiner et al. 1993). Experiments designed to disrupt FAK signaling, with overexpression of a kinase-dead FAK mutant, dominant negative FAK-CD or a small interfering RNA–induced silencing of the expression of FAK, resulted in reduced cell proliferation, viability and increased cell death (Hauck et al. 2002, Han et al. 2004). Therefore, it is timely to pinpoint FAK in the onset and progression of cancer.

Molecular Structure of Focal Adhesion Kinase

Focal adhesion kinase (FAK), also known as protein tyrosine kinase 2 alpha (PTK2a), is a non-receptor tyrosine kinase that resides at focal adhesion protein clusters (Fiodorek et al. 1995). The FAK protein has a molecular mass of 125kDa and is encoded by the FAK gene located on human chromosome 8q24.This protein consists of an amino-terminal regulatory FERM (band 4.1, ezrin, radixin, moesin homology) domain, a central catalytic kinase domain, two proline-rich motifs, and a carboxy-terminal focal adhesion-targeting (FAT) domain (Figure 1-1).

Closely related to the FAK, PTK2b, proline-rich tyrosine kinase 2 (PYK2), is also located on human chromosome 8p22-p11.2 and shares a similar domain structure with FAK (Manning et al. 2002). The FERM and FAT domain regions have around 40% and the kinase domain 60% conserved amino acid sequences. Although FAK is ubiquitously expressed in all tissues and cell types, the Pyk2 is expressed primarily in hematopoietic and neuronal cell types (Avraham et al. 2000, Orr et al. 2004).

The amino acid sequence of FAK is more than 90% homologous between human, chicken, mouse and frog, suggesting it has a critical role in signal transduction and regulation among

species (Corsi et al. 2006). The expression of the human FAK gene is regulated by a 600 base pair promoter region that contains many transcription binding sites including AP-1, AP-2, SP-1, PU.1, GCF, TCF-1, EGR-1, NF-kappa B and p53 (Golubovskaya et al. 2004). NF-kappa B induces the transcription of FAK whereas p53 blocks FAK promoter and inhibits its activity. FAK mRNA and protein levels increase from embryonic day 7.5 and FAK-null embryos die at day 8.5 during mouse development, indicating that FAK is essential in embryonic development (llik et al. 1995). Pathological analysis of FAK-null embryos demonstrated mesodermal defects; involution of head mesenchyme, and absence of notochord or somite was formation.

Activation and Signaling Through FAK

FAK is a multi functional protein that has a kinase activity as well as serving as a scaffold protein. In the focal adhesion complex, FAK exists in its inactive state by masking the catalytic cleft with its FERM domain (Cooper et al. 2003). Interaction with integrins and growth factor receptors as well as intracellular kinases cause a conformational change in FAK and allow autophosporylation of the Y397 site, which leads to additional phosphorylation and full activation of FAK. The Y397 phosphorylated tyrosine creates a binding site for the SH2 domain of Src family kinases. SH2 domain binding of Src to the FAK releases Src Y527 auto-inhibitory interaction and leads to the activation of Src (Figure 1-1). In return, activated Src phosphorylates additional sites on FAK, including residues Y576 and Y577 in the kinase activation loop, promoting further increased catalytic activity of FAK. The activated FAK/Src complex then initiates a cascade of phosphorylation events and new protein-protein interactions to trigger numerous signaling pathways. These FAK signaling pathways have been shown to regulate a variety of cellular functions in both normal and cancer cells (Figure 1-2).

FAK as a Target for Therapy

Recently, several reports described the properties of FAK inhibitors, and FAK has been proposed to be a new therapeutic target (McLean et al. 2005). Initial studies, which evaluated the effects of FAK inhibition in preclinical models focused on dominant negative mutants of FAK, antisense oligonucleotides and siRNAs (Parsons et al. 2008). More recently, scientists at Novartis Pharmaceuticals designed and synthesized a series of 2-amino-9-aryl-7H-pyrrolo [2,3-d] pyrimidines to inhibit FAK kinase activity (Choi et al. 2006). Chemistry was developed to introduce functionality onto the 9-aryl-ring, which resulted in the identification of potent FAK inhibitors. Others and we have published reports on the use of such FAK inhibitors that have targeted the ATP binding site in the kinase domain. In human pancreatic cancer, we have shown widespread expression of FAK in primary pancreatic adenocarcinoma. In addition, we have shown significant upregulation of FAK protein expression in metastatic lesions. In human pancreatic cancer cells, we showed that the FAK kinase inhibitor, TAE226, decreases viability, increases cell detachment and increases apoptosis (Liu et al. 2008). Other studies have shown that TAE226 readily induced apoptosis in human breast cancer cells with overexpressed Src or EGFR. Of note, these cells were resistant to adenoviral FAK dominant negative treatment, indicating that kinase inhibition was important for dowregulation of FAK function and the observed phenotypic changes (Golubovskaya et al. 2008).

Subsequent studies have analyzed the *in vivo* effects of TAE226. In a subcutaneous model of human esophageal cancer, TAE226 given orally at 30 mg/kg significantly decreased tumor volume and weight compared to placebo (Watanabe et al. 2008). Similar results from *in vivo* studies have confirmed the ability of TAE226 to decrease the growth of ovarian and glioma xenografts (Shi et al. 2007). We have also used this inhibitor in other cancer cell lines including pancreatic cancer cells and found that this inhibitor can effectively cause apoptosis.

While initial results with inhibition of kinase activity of FAK has shown anti-neoplastic effects, TAE226 has been shown to also inhibit the activity of IGF-1R at nanomolar concentrations (Liu et al. 2007). Therefore, the activities against multiple tumor types likely reflect its dual inhibition of adhesion and growth promoting pathways. However, cross-reactivity with other kinases may increase toxicity. Recently, Pfizer pharmaceuticals have published results on an ATP competitive reversible inhibitor of FAK that has bioavailability suitable for preclinical animal and human studies (Roberts et al. 2008). It also cross-reacts with Pyk2. PF-562, 271 was shown to exhibit >100 fold selectivity for FAK when assayed against a panel of unrelated kinases. Treatment of cancer cell lines showed a dose dependent decrease in FAK phosphorylation at the Y397 site. The IC_{50} for FAK phosphorylation was reported to be 5 nmol/L. Antitumor efficacy was observed in mice subcutaneous xenograft models with minimal weight loss or mortality (Roberts et al. 2008).

PF-562, 271 is currently in phase II clinical trials. Phase 1 study results with this drug in patients with advanced solid malignancy have been reported in abstract form (Siu et al. 2007). Studies have been performed in two centers in the United States and one center in Canada and Australia with oral dosing as a single agent. Thirty-two patients received from 5 mg up to 105 mg twice a day. Adverse events possibly related to the drug in over 10% were nausea, vomiting, fatigue, anorexia, abdominal pain, diarrhea, headache, sensory neuropathy, rash, constipation and dizziness. Adverse events were generally grade 1-2 and reversible. Doses over 15 mg twice a day produced steady state plasma concentrations exceeding target efficacious levels predicted from preclinical models. Prolonged disease stabilization was observed in several tumor types. Phase 1 results indicated good tolerability to this drug with favorable pharmacokinetics and

pharmacodynamics (Siu et al. 2007). This drug represents the sole FAK inhibitor being tested in humans to date.

Another approach to inhibit FAK function can be to target protein-protein interactions between FAK and its binding partners such as p53, IGF-1R, VEGFR-3 or EGFR or targeting sites of FAK phosphorylation (Golubovskaya et al. 2008, Zheng et al. 2009, Kurenova et al. 2009). Tyrosine 397 is an autophosphorylation site of FAK that is a critical component in downstream signaling, providing a high-affinity binding site for the SH2 domain of Src family kinases. Y397 is also a site of binding of PI3 kinase, growth factor receptor binding Grb-7, Shc and other proteins. Thus, the Y397 site is one of the main phosphorylation sites that can activate FAK signaling in cells. It was recently demonstrated that computer modeling and screening can be performed to identify novel small molecules that inhibit protein-protein interactions at the Y397 site (Golubovskaya et al. 2008). In this approach, more than 140,000 small molecule compounds were docked into the N-terminal domain of the FAK crystal structure in 100 different orientations. Those compounds with the greatest energy of interaction based on van der Waals and electrostatic charges were identified as lead compounds. One compound, 1,2,4,5-benzenetetraamine tetrahydrocholoride (Y15) significantly decreased viability in most cancer cells and specifically and directly blocked phosphorylation of Y397-FAK in a dose and time dependent manner. Furthermore, it inhibited cell adhesion and effectively caused breast tumor regression *in vivo* (Golubovskaya et al. 2008). Finally, we have shown that it inhibits pancreatic cancer growth *in vivo* both alone and in combination with gemcitabine chemotherapy (Hochwald et al. 2009).

One potential advantage of our approach to identify small molecules through in silico screening is increased target specificity. Y15 did not affect phosphorylation of the FAK

homologue, Pyk-2, which can be explained by only 43% amino acid identity between N-terminal domains of FAK and Pyk-2. Other kinase inhibitors of FAK have shown inhibition of Pyk-2 autophosphorylation and likely are less specific for inhibition of FAK function.

The Insulin-like Growth Factor Receptor

The insulin-like growth factor (IGF) signaling system also plays an important role in the formation and progression of human cancer. Deregulation of the IGF pathways, such as the overexpression and over-activation of insulin-like growth factor-1 receptor (IGF-1R) is a common event in several malignancies (Vincent et al. 2002). Mature IGF-1R is a heterotetramer consisting of two α subunits and two β subunits. The β subunit contains a transmembrane domain, a juxtamembrane domain, a tyrosine kinase domain and a C-terminal tail. Initiated by ligand binding, IGF-1R undergoes conformational changes and autophosphorylation that trigger an intracellular signaling cascade including activation of the mitogen-activated protein kinase (MAPK) and the phosphatidylinositol 3 kinase (PI3K) pathways, two main downstream signals of IGF-1R (Dews et al. 2000). IGF-1R signaling is required for cellular transformation by most oncogenes and facilitates the survival and spread of transformed cells (Valentinis et al. 1999). Interruption of IGF-1R signaling has been shown to inhibit tumor growth and block metastasis in a wide variety of tumor models (Pollak et al. 2008).

IGF-1R and Signaling Pathways

Both the IGF-1 and insulin receptors are heterotetrameric transmembrane glycoproteins with intrinsic tyrosine kinase activity. Following ligand binding, both receptors undergo phosphorylation and thus activate insulin receptor substrate-1 (IRS-1), which then initiates a cascade of events that have mitogenic and metabolic effects (Vincent et al. 2002). Insulin, unlike IGF-1, is produced by the beta cells of the Islet of Langerhans and is primarily involved in glucose homeostasis and the regulation of metabolic pathways. The role of insulin in

tumorigenesis is less clear; in pancreatic cancer, its effect appears to be its ability to activate the IGF-1 receptor (Korc et al. 1998).

The best-defined pathway by which IGF-1R signaling can prevent apoptosis is mediated by signaling from phosphoinositide 3-kinase (PI3K) to Akt. Tyrosine phosphorylation of IRS-1 by IGF-1R leads to PI3K activation as a result of binding its regulatory subunit through the SH2 domain to IRS-1 and subsequent increase in phosphatidylinositol 3,4,5-trisphosphate (PIP3). The proteins Akt/PKB and phosphoinositide-dependent kinase-1 (PDK-1) are then bound by PIP3. Residue Thr308 on Akt/PKB is then phosphorylated by PDK-1. Activated Akt/PKB plays a key role in the prevention of apoptosis. It phosphorylates and inactivates several proapoptotic proteins including Bad (Bcl-2 family member). Akt/PKB also can prevent the initiation of the caspase cascade through phosphorylation and inactivation of caspase-9. In addition to the inhibition of pro-apoptotic transcription factors, the activity of Akt/PKB also increases the levels of anti-apoptotic proteins including Bcl-2 and Bcl-X. With activation of Akt/PKB, the expression of the anti-apoptotic transcription factor NF-kB is also increased (Vincent et al. 2002).

There is evidence of Akt involvement in human malignancies. Akt was found to be amplified 20-fold in primary gastric adenocarcinoma. Additional studies have shown genomic amplification and overexpression of Akt in several pancreatic cancer cell lines. Of particular note is the fact that overexpression of Akt occurs more frequently in undifferentiated, and thus more aggressive, tumors. It has been shown that MAPK can also influence Akt phosphorylation, contributing to tumor cells resistance to apoptosis (Staal et al. 1998, Ruggeri et al. 1998).

The mitogen-activated protein (MAP) kinases are also activated by IGF-1R and are involved in the regulation of apoptosis in different cell types (Dews et al. 2000). One principal MAPK pathway involves the extracellular signal-regulated kinase (ERKs) ERK1 and ERK2. Upon IGF-1R autophosphorylation, the protein Shc is recruited to the IGF-1 receptor and becomes phosphorylated on tryosine residues. Activated Shc then binds the adaptor Grb2 in an IRS-1 independent manner, leading to activation of the Ras-ERK pathway (Kim et al. 1998). This pathway has been shown to be important in fibroblasts in regulating the machinery of apoptosis in detachment-induced death or anoikis (Valentinis et al. 1999). Similar to the Akt pathway, the downstream target of ERK might prevent apoptosis through Bad inactivation.

IGF-1R and Cancer

Several members in the IGF-family signaling pathway, including IGF-1, IGF-1R, IGF-2R and IRS-1 are overexpressed in cancer including pancreatic malignancy (Stoeltzing et al. 2003, Bergmann et al. 1995, Bergmann et al. 1996, Ishiwata et al. 1997). Several studies support the significance of the IGF-1 receptor-mediated mitogenic signal in cancer cells. Both IGF-1 receptor antisense oligonucleotides and anti-IGF-1R antibodies have been shown to inhibit the proliferation of human pancreatic cancer cells. Overexpression of IRS-1 in pancreatic cancer contributes to increased activation of the IGF-1R signaling pathway (Bergmann et al. 1995, Bergmann et al. 1996).

Interaction Between FAK and IGF-1R

Our laboratory has demonstrated by co-immunoprecipitation and confocal microscopy studies that FAK and IGF-1R physically interact in human cancer cells and that these cells have survival signals operative through FAK and IGF-IR activities. As shown in figure 1-3, the kinase domain of IGF-1R□ directly interacts with the NT2 region (aa 126-243) of FAK-FERM domain. In addition, our lab has shown that dual inhibition of both kinases synergistically induces cell

detachment, decreases cell viability and increases apoptosis, which was demonstrated by multiple approaches in fibroblast and cancer cells with the use of multiple inhibitors including transient expression of a dominant negative FAK (Ad FAK-CD), FAK knockdown with siRNA, stable expression of an IGF-1R dominant negative, a selective small molecule inhibitor of IGF-1R (AEW-541) and a novel small molecule kinase inhibitor of both FAK and IGF-1R TAE226 (Liu et al. 2008). The mechanism for this synergistic effect appears to be through pathways that involve ERK and Akt. Both p-ERK and p-Akt were decreased following dual inhibition of FAK and IGF-1R.

The strategy of dual FAK and IGF-1R kinase inhibition has been shown to be effective in tumor models involving several human malignancies. The FAK and IGF-1R kinase inhibitor (TAE226) was shown to inhibit growth of human ovarian carcinoma cell lines in a time and dose dependent fashion. TAE226 significantly reduced tumor growth *in vivo* both when administered alone and when given concomitantly with docetaxel chemotherapy. The therapeutic efficacy was related to reduced pericyte coverage, induction of apoptosis of tumor-associated endothelial cells and reduced microvessel density and tumor cell proliferation (Halder et al. 2007). In addition, TAE226 was shown to inhibit human glioma cell growth as assessed by a cell viability assay and attenuated G(2)-M cell cycle progression associated with a decrease in cyclin B1 and phosphorylated cdc2 protein expression. TAE226 treatment significantly increased the survival rate of animals in an intracranial glioma xenograft model (Liu et al. 2007). Finally, TAE226 was found to induce apoptosis in human breast cancer cells that overexpressed Src or EGFR (Goluboyskoya et al. 2008).

Dual Inhibition of FAK and IGF-1R

FAK inhibition: While emerging data strongly suggests that FAK is an excellent target for developmental therapeutics of cancer, specific small molecule kinase inhibitors of FAK have

been difficult to obtain (McLean et al. 2005, Van Nimwegen et al. 2007). Three such kinase inhibitors were reported from Novartis (NVP-TAE 226) and Pfizer (PF-573, 228 and PF-562, 271), but only PF-562, 271 is in clinical trials in cancer patients (Shi et al. 2007, Slack-Davis et al. 2007, Roberts at al. 2008).

IGF-1R inhibition: Industry leaders are exploring the utility of antibodies to the extracellular domain of IGF-1R. These antibodies are under investigation in multiple tumor types. Six companies are currently testing small molecule inhibitors targeting the IGF-1R tyrosine kinase (Hewis et al. 2009, Pollak et al. 2008).

Disruption of Protein-Protein Interactions

Up to the present, the approach to dual FAK and IGF-1R inhibition was based on inhibiting their kinase activities. Due to sequence homology, particularly in the kinase domain, and structural similarity of IGF-1R to other receptors such as the insulin receptor, the main problem with kinase inhibitors is their lack of specificity. Approaches of targeting the ATP competitive binding site lack specificity for IGF-1R or FAK inhibition. In addition, it frequently appears that disruption of the kinase domain does not specifically interfere with the downstream signaling of FAK or IGF-1R and it is unclear whether the kinase function or the scaffolding function of these proteins is more important. Targeting FAK protein-protein interaction sites represents a novel approach to FAK inhibition and it was developed in the Cance/Hochwald laboratory and proven by developing a FAK-VEGFR3 inhibitor C4 (Kurenova et al. 2009). There have been no previous studies, which have examined applicability of this strategy to FAK and IGF-1R protein interactions targeting in human cancer cells. Small organic molecules are particularly attractive as inhibitors of intracellular protein–protein interactions because of the ability to modify their structures to achieve optimal target binding, and because of their ease of delivery in *in vivo* systems.

Targeted Cancer Types

Both FAK and IGF-1R are expressed in varying amount in several cancer types. For our study, we focused on melanoma, esophageal and pancreatic cancers to study the effects of disruption of FAK and IGF-1R. The rationale to target these cancer types is that they are refractory to most standard therapies and are associated with high cancer mortality rates.

Melanoma

Cutaneous melanoma is one of the cancers with the greatest incidence in the last 50 years. Melanoma patients with metastatic disease have a very poor prognosis with a 5-year survival probability of less than 5%. This is largely due to the failure of chemotherapy or immunotherapy treatments to impact advanced disease (Eggermont et al. 2009). Researchers have demonstrated that progression from benign nevi to malignant melanoma is paralleled by an increased expression of FAK and IGF-1R (Kanter-Lawensohn et al. 1998, Kanter-Lawensohn et al. 2000, Kahana et al. 2002). The MAPK and PI3K-Akt signaling pathways are constitutively activated through multiple mechanisms in melanoma and plays a major role in tumor progression. It has recently been shown that aggressive melanoma cell lines are resistant to both MEK and PI3K inhibitors when administered alone, whereas the combination of MEK with PI3K inhibitors suppresses melanoma growth and invasion (Jaiswal et al. 2009).

In this study, I demonstrate a unique approach to melanoma therapy by inhibiting FAK and IGF-1R function through specific targeting of the site of their protein-protein interaction. This study demonstrates that I can inhibit downstream signaling from these tyrosine kinases by targeting their binding site resulting in inhibition of tumor growth in both *in vitro* and *in vivo* models.

Esophageal Cancer

Esophageal cancer is one of the deadliest cancers worldwide, yet studied the least (Jemal et al. 2003). Worldwide, esophageal cancer is the sixth leading cause of death from cancer (Pisani et al. 1999). According to the National Cancer Institute estimate in 2009, in the United States, there were approximately 16,500 new cases of esophageal cancer and nearly 14,500 esophageal cancer deaths, making esophageal cancer one of the most deadly of all cancers (http://www.cancer.gov/cancertopics/types/esophageal/). By the time esophageal cancer is diagnosed, >50% of patients have either unresectable tumors or radiographically visible metastases. It is very likely therefore; the 5-year survival rate for all esophageal cancer patients is approximately 10-15%.

Strong expression of FAK was found in 94.0% of Barrett's esophageal adenocarcinoma compared with 17.9% of Barrett's epithelia, suggesting that FAK might play a critical role in the progression of Barrett's esophageal adenocarcinoma. When esophageal adenocarcinoma cells were treated with the dual FAK and IGF-1R kinase inhibitor, TAE226, cell proliferation and migration were greatly inhibited with an apparent structural change of actin fiber and a loss of cell adhesion. The activities of FAK, IGF-IR, and AKT were suppressed by TAE226 and subsequent dephosphorylation of BAD at Ser (136) occurred, resulting in caspase-mediated apoptosis (Watanabe et al. 2008). Both IGF-IR and its ligands are overexpressed in esophageal cancer tissues compared with the normal ones (Mori et al. 1996, Liu et al. 2002, Ouban et al. 2003). Kalinina et al. examined IGF-1R expression in 234 esophageal tumors and detected over expression of the IGF-1 receptor in 121 of the tumors (52%). They also identified a correlation between the over expression of IGF-1R and reduced overall survival for adenocarcinoma (P=0.05) patients. Subsequently, evaluation of a new tyrosine kinase inhibitor of IGF-IR, NVP-AEW541, on the signal transduction and the progression of of gastrointestinal (GI) cancers

demonstrated that inhibition of IGF-1R suppressed proliferation and tumorigenicity *in vitro* and *in vivo* in a dose-dependent manner (Piao et al. 2008).

Pancreatic Cancer

Pancreatic cancer ranks 13th in incidence, but 8th as a cause of cancer death worldwide. In the United States, pancreatic cancer is the fourth leading cause of cancer death in both men and women. Every year, nearly 30,000 Americans die of pancreatic cancer, which accounts for 22% of gastrointestinal cancer deaths and 5% of all cancer deaths (Jemal et al.2004).

There is no effective therapy for pancreatic cancer besides surgical resection. Unfortunately, only a minority of patients are candidates for potentially curative surgery as the tumor spreads early to extrapancreatic sites. Patients with metastatic pancreatic cancer survive less than 1 year following diagnosis. The current challenge for both clinicians and scientists is to translate the growing body of knowledge of the molecular basis of this disease into effective strategies for early diagnosis and systemic treatment.

Molecular Abnormalities in Pancreatic Cancer

The pancreatic ducts are one of the most common sites of human neoplasia, affecting nearly half of the elderly population (Kloppel et al. 1980, Kozuka et al. 1979, Pour at al. 1979). Just as multiple adenomas can occur within the colorectum of an individual, multiple independent benign pancreatic neoplasms tend to be present simultaneously. Only about 1-in-500 intraductal neoplasms progresses to cancer, and appears to do so through a series of progressive lesions (Frukawa et al. 1994). The tumor progression model for pancreatic neoplasia therefore follows closely upon the model established for colorectal tumors.

Molecular studies of pancreatic duct carcinomas have revealed that this cancer is associated with several genetic mutations. Current genetic profiles of pancreatic cancer detail are amongst the highest number of gene mutations, per tumor, for any human system known. These

mutations include very frequent mutations of the K-ras gene leading to its activation, inactivation of the p16 gene, as well as common inactivations of the p53 and DPC4 genes (Blanck et al. 1999, Almoguera at al. 1988, Caldas et al. 1994). Other alterations that occur in pancreatic cancer include deregulation of growth factors and growth factor receptors, matrix metalloproteinases and regulators of tumor angiogenesis. In addition, amplification of genes from the 8q, 11q, 17q and 20q chromosome arms is common in pancreatic cancer (Mahlamaki et al. 2002).

Data from our laboratory has shown increased expression of FAK and IGF-1R in human pancreatic cancers as they progress from normal pancreas to adenocarcinoma and subsequently to metastases (Zheng et al. 2010). Therefore, FAK and IGF-1R appear to be valid targets in pancreatic cancer.

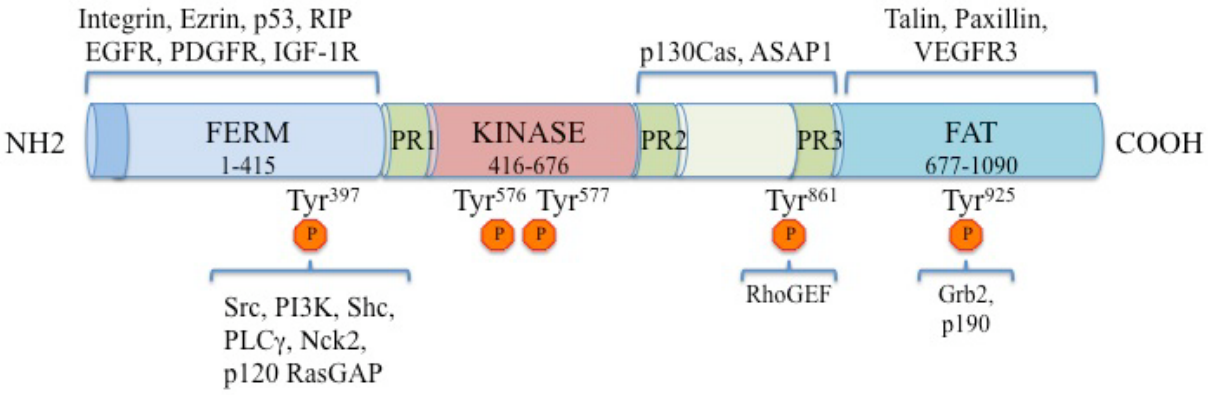

Figure 1-1. FAK structure and interacting proteins. FAK protein is composed of an amino-terminal regulatory FERM (band 4.1, ezrin, radixin, moesin homology) domain, a central catalytic kinase domain, two proline-rich motifs, and a carboxy-terminal focal adhesion-targeting (FAT) domain. Interaction with integrins and growth factor receptors as well as intracellular kinases cause conformational changes in FAK and allow autophosporylation of the Y397 site, which leads to additional phosphorylation and its full activation. Once it is activated, phoshorylated tyrosine sites of FAK create a binding site for the SH2 domain of Src family kinases. SH2 domain binding of Src to FAK releases Src Y527 auto-inhibitory interaction and leads the activation of Src. In return, activated Src phosphorylates additional sites on FAK, including residues Y576 and Y577 in the kinase activation loop, promoting further increased catalytic activity of FAK (Ucar et al. in press).

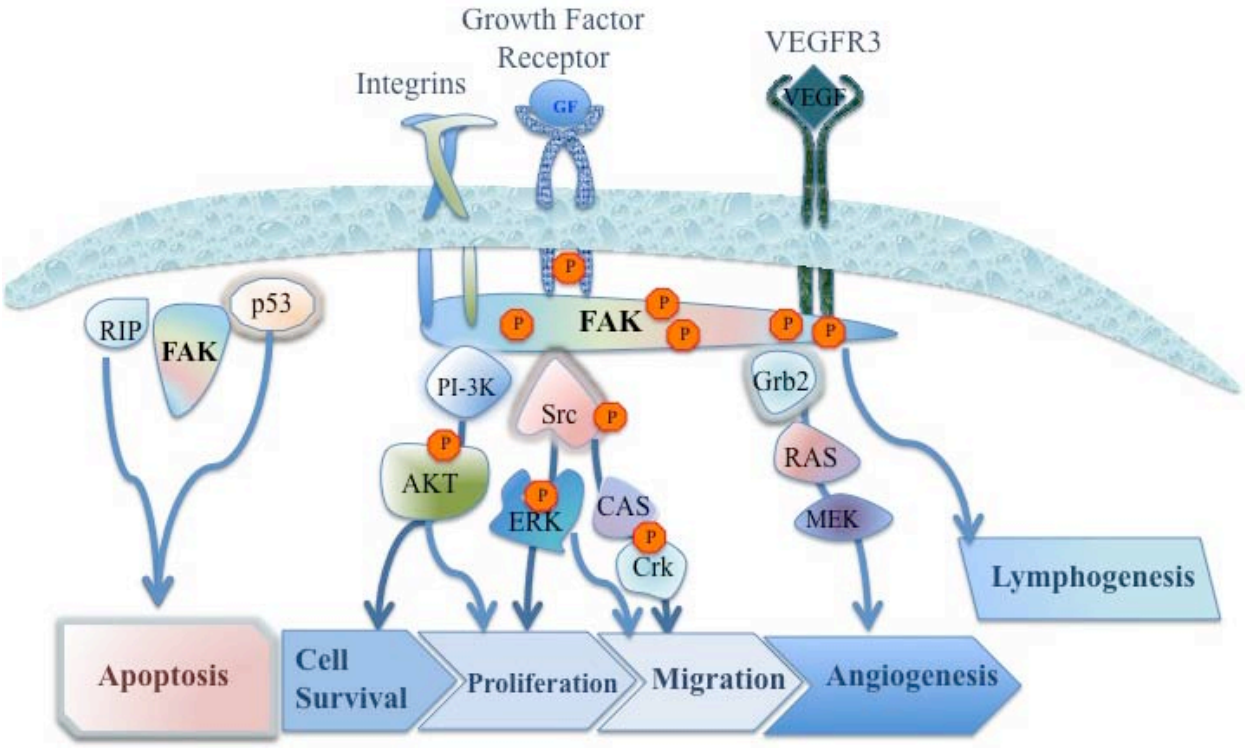

Figure 1-2. FAK signaling. Schematic diagram of FAK interacting proteins and signaling cascades that are involved in apoptosis, cell survival, proliferation, migration, angiogenesis and lymphogenesis (Ucar et al. in press). Interaction with integrins and growth factor receptors as well as intracellular kinases cause a conformational change in FAK and allow autophosporylation of the Y397 site, which leads to additional phosphorylation and full activation of FAK. The Y397 phosphorylated tyrosine creates a binding site for the SH2 domain of Src family kinases. SH2 domain binding of Src to the FAK releases Src Y527 auto-inhibitory interaction and leads to the activation of Src. In return, activated Src phosphorylates additional sites on FAK, including residues Y576 and Y577 in the kinase activation loop, promoting further increased catalytic activity of FAK. The activated FAK/Src complex then initiates a cascade of phosphorylation events and new protein-protein interactions to trigger numerous signaling pathways.

CONSTRUCT	AMINO ACIDS	FERM DOMAIN STRUCTURE	FUNCTION IN FAK
FAK-NT1	1-126	Subdomain A: ubiquitin-like fold	
FAK-NT2	126-243	Subdomain B: four-helix bundle or acyl coenzyme A binding protein	Binding kinase domain, FAK
FAK-NT3	243-415	Subdomain C: phosphotyrosine-binding-like domain or PH/PTB/EVH1	D395 PI3K and Grb7 binding Y397 Src and PTEN binding, Y407

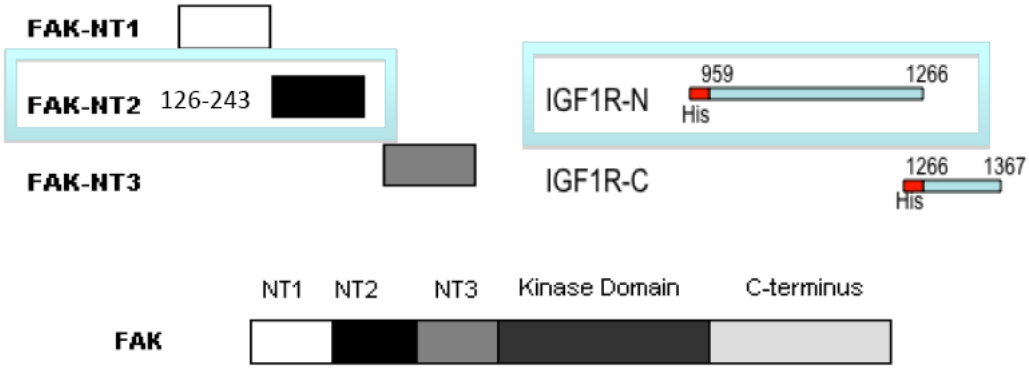

Figure 1-3. FAK constructs and the domains of interaction between FAK and IGF-1R.

CHAPTER 2
MATERIALS AND METHODS

Cell Lines and Cell Culture

Melanoma Cell Lines

A375, SK-MEL-28 cells were obtained from American Type Culture Collection (Rockville, MD). A375 and SK-MEL-28 cells were maintained in Dulbecco's modified Eagle's medium supplemented with 10% fetal bovine serum (FBS) and 1 µg/ml penicillin–streptomycin. The C8161 cell lines, kindly provided by Dr. William Cance (The Roswell Park Cancer Institute, Buffalo, NY), were maintained in RPMI 1640 supplemented with 10% FBS, 1 µg/ml penicillin–streptomycin. Melanocytes were obtained from Lifeline Cell Technology (Walkersville, MD) and maintained in DermaLife® M Melanocyte Culture Medium (Lifeline Cell Technology, Walkersville, MD). All cell lines were incubated at 37°C in a 5% CO2 humidified incubator.

Esophageal Cancer Cell Lines

TE and KYSE group cell lines kindly provided by Dr. Yutaka Shimada (University of Toyama, Toyama, Japan). Esophageal cancer lines were maintained in RPMI 1640 supplemented with 10% FBS, 1 µg/ml penicillin–streptomycin. All cell lines were incubated at 37°C in a 5% CO_2 humidified incubator.

Pancreatic Cancer Cell Lines

As-PC1, Bx-PC3, Panc-1 and MiaPaca-2 cells were obtained from American Type Culture Collection (Rockville, MD). Panc-1 cells were maintained in Dulbecco's modified Eagle's medium supplemented with 10% fetal bovine serum (FBS) and 1 µg/ml penicillin–streptomycin. MiaPaca-2 cells were maintained in Dulbecco's modified Eagle's medium supplemented with 10% FBS, 2.5% horse serum and 1 µg/ml penicillin–streptomycin. The As-PC1 and Bx-PC3 cell lines were maintained in RPMI 1640 supplemented with 10% FBS, 1 µg/ml penicillin–

streptomycin. Human pancreatic duct epithelial (HPDE) cells were kindly provided by Dr. Carol Otey (University of North Carolina, Chapel Hill, NC) and maintained in Keratinocyte-SFM Serum free medium (Gibco/Invitrogen, Carlsbad, CA) supplemented with L-Glutamine, EGF&BPE and soy bean trypsin inhibitor (Gibco/Invitrogen, Carlsbad, CA). All cell lines were incubated at 37°C in a 5% CO2 humidified incubator.

Other Cell Lines

FAK knockout mouse embryonic fibroblast cells (FAK -/- MEFs) were kindly provided by Dr. William Cance (Roswell Park, Buffalo, NY) and maintained in Dulbecco's modified Eagle's medium supplemented with 10% fetal bovine serum (FBS) and 1 µg/ml penicillin–streptomycin. IGF-1R knockout mouse embryonic fibroblast cells (IGF-1R-/- MEF) were kindly provided by Dr. Renato Baserga (Kimmel Cancer Center, Thomas Jefferson University, Philadelphia, PA) and maintained in Dulbecco's modified Eagle's medium supplemented with 10% fetal bovine serum (FBS) and 1 µg/ml penicillin–streptomycin. IGF-1R-/- clones were selected by using 200 mg/ml of Hygromycin B. MCF7, MCF10A and BT474 cells were purchased from American Type Culture Collection (ATCC, Rockville, MD). BT474 were maintained in RPMI-1640 with 10% fetal bovine serum and insulin 250 ug/ml. MCF7 cells were maintained with Modified minimum Eagle’s media with 10% fetal bovine serum, 1X non-essential amino acids (Cellgro, Herndon, VA), 1 mM sodium pyruvate, and 500µg/ml insulin. MCF10A, an immortalized human mammary epithelial cell line was cultured in a 1:1 mixture of Dulbecco's modified Eagle's medium and F12 medium (DMEM-F12) supplemented with 5% horse serum, hydrocortisone (0.5 µg/ml), insulin (10 µg/ml), epidermal growth factor (20 ng/ml), and penicillin-streptomycin (100 µg/ml each).

Reagents and Antibodies

MTT reagent was purchased from Promega (Madison, WI). CFSE was purchased from Molecular Probes (Eugene, OR). TAE226 was obtained from Novartis (East Hanover, NJ). Gemcitabine (Gemzar) was purchased from Eli Lilly (Indianapolis, IN). 5-Fluorouracil (5-FU) was supplied by Sigma-Aldrich Chemical (Poole, UK). Recombinant Human IGF-I was purchased from R&D (Minneapolis, MN). Anti-FAK monoclonal (4.47) and anti-phospho-tyrosine monoclonal (4G10) antibodies were obtained from Upstate (Lake Placid, NY). Anti-FAK (C20) antibody and anti-IGF-1Rβ antibody (C20) were obtained from Santa Cruz Biotechnology (Santa Cruz, CA). Anti-His antibody and anti-GST antibody were obtained from Sigma (Saint Louis, MS). Anti-phospho-IGF-1R and anti-IGF-1R antibodies were from Calbiochem (San Diego, CA). Anti-phospho-FAK (Tyr397) and anti-phospho-Src antibody were from Biosource (Camarillo, CA). Anti-src, anti-caspase 8, anti-caspase 9, anti-phospho-Akt, anti-Akt, anti-phospho-ERK1/2, anti-ERK1/2, were from Cell Signaling Technology (Beverly, MA). Anti-caspase 3/7 and anti-PARP antibodies were from BD Biosciences (Catalogue #611038, San Jose, CA). This PARP antibody recognized the full length, uncleaved form of PARP. Anti-β-actin antibodies were from Sigma (St Louis, MO). Anti-glyceraldehyde 3-phosphate dehydrogenase (GAPDH) antibody was from Advanced ImmunoChemical (Long Beach, CA).

Cell Viability (MTT) and CFSE Proliferation Assay

Cells were plated in 96-well plates and let adhere overnight. After cell treatment, cell viability was measured by 3-(4,5-dimethylthiazol-2-yl)-2,5-diphenyl tetrazolium bromide (MTT) assay (CellTiter 96® AQueous). Briefly, 20 µl of the tetrazolium compound was added to each well. The cells were then incubated at 37°C for 1 h. The plate was read at 490 nm with a plate reader to determine the viability. In detachment assays, detached and attached cells were

harvested separately and counted in a hemocytometer. The percentage of detachment was calculated by dividing the number of detached cells by the total number of cells.

For staining with CFSE (CF(DA)SE, 5,6-carboxy fluorescein diacetate succinimidyl ester), 1×10^7/ml cells were suspended in PBS and incubated at 37 °C for 5 min with the 10 μM of CFSE. Staining was terminated by adding culture medium. The cells were washed once in PBS, resuspended in culture medium and 5×10^5 cells plated. Stained cells were cultured with medium alone or with compound for 24, 48, and 72 hours, fixed and analyzed by a FACS Calibur cytometer (Becton Dickinson, San Jose, CA). Unstained cells were included in all experiments and were used to set the conditions on the flow cytometer.

Computational Docking

The crystal structures of the N-terminal domain of FAK (PDB code 2AL6) and the kinase domain of IGF-1R (PDB 1P40A) were utilized for *in silico* molecular modeling of their interaction as previously described (Ceccarelli et al. 2006, Munshi et al. 2002). The three-dimensional coordinates of compound NSC344553, obtained from the database of the National Cancer Institute, Developmental Therapeutics Program (NCI/DTP), were docked onto the predicted interface of the amino-terminus of FAK (amino acids 127-243) with the intracytoplasmic portion of IGF-1R (Zheng et al. 2009). All docking calculations were performed with the University of California-San Francisco DOCK 5.1 program, using a clique-matching algorithm to orient small molecule structures with sets of spheres that describe the target sites on FAK (Hewish et al. 2009). 100 orientations were created for NSC344553 in the target site and were scored using the computer program grid-based scoring function. Docking calculations were performed on the University of Florida High Performance Computing supercomputing cluster using 16 processors (http:hpc.ufl.edu). The intermolecular energies for all configurations of NSC 344553 in binding to FAK-NT2 were calculated as the sum of

electrostatic and van der Waals energies. These energy terms were evaluated as correlation functions, which were computed efficiently with Fast Fourier Transforms.

Production of GST-Fusion Proteins

The FAK-GST plasmid constructs (pGEX vector) were kindly provided by Dr. Elena Kurenova (Roswell Park Cancer Insititute, Buffalo, NY). His-tagged IGF-1R protein was purchased from Blue Sky Biotechnology (Worchester, MA). The GST-fusion proteins (FAK fragments) were expressed in BL21 (DE3) Escherichia coli bacteria by incubation with 0.2 mM isopropyl b-D-galactopyranoside (IPTG) for 6 h at 37 °C. The bacteria were lysed by sonication, and the fusion proteins were purified with glutathione-Sepharose 4B beads (GE Healthcare, NJ).

Pull-Down Assay

For the pull-down binding assay, His-tagged IGF-1R fragment protein (200 ng) were precleared with GST immobilized on glutathione-Sepharose 4B beads by rocking for 1 h at 4 °C. The precleared His-tagged protein was incubated with 0.2 μg of GST-FAK fusion protein immobilized on the glutathione-Sepharose 4B beads for 1 h at 4 °C and then washed three times with PBS. Equal amounts of GST-fusion proteins were used for each binding assay. Bound proteins were boiled in 6× Laemmli buffer and analyzed by SDS–PAGE and Western blotting.

Immunoprecipitation and Western Blotting

Cells were washed twice with ice cold 1x phosphate-buffered saline (PBS) and lysed on ice for 30 min in buffer containing 20 mM Tris, pH 7.4, 150 mM NaCl, 1% NP-40, 5 mM ethylenediaminetetraacetic acid, protease inhibitors (CompleteTM Protease Inhibitor, Roche, NJ) and phosphatase inhibitors (Calbiochem, CA). The lysates were centrifuged at 13,000 r.p.m. for 30 min at 4°C and the supernatants were collected. Protein concentration was determined using Bio-Rad Protein Assay. For immunoprecipitation, 100-200 μg of total cell extract was used for each sample. The extracts were incubated with 1 μg of antibody overnight at 4°C. Twenty-five

microliters of protein A/G-agarose beads (Oncogene Research Products, CA) were added and the samples were incubated with rocking for an additional 2 h at 4°C. The precipitates were washed four times with lysis buffer, resuspended in 30 µl Laemmli buffer. For western blotting, boiled samples containing 30 µg of protein were resolved by SDS–PAGE followed by transferring to polyvinylidene difluoride membrane (Bio-Rad, CA). The immunoblots were developed with the Western LightningTM Chemiluminescence Reagent Plus (Pierce Thermoscientific, Rockford, IL). The intensity of the bands in the western blots was measured with scion image analysis software program.

Short Hairpin RNA Transfection of Cells

Control shRNA (mock) and FAK shRNAs was obtained from Open Biosystems. The sequences of short hairpin RNAs against human FAK were: (5'-CCGGCCGATTGGAAACCAACATATACTCGAGTATATGTTGGTT TCCAATCGTTTTG-3'; 5'-CCGGGCCCAGAAGAAGGAATCAGTTCTCGAG AACTGATTCTTCTTCTGGGCTTTTTG-3') and control shRNA (mock) (5'- TCCGAACGTGTCACGTTCTCTTGAAACGTGACACGTTCGGAGA-3'). For the transfection of cells ($2x10^5$ cells/well) were seeded into 6-well plates in 2 ml medium one day prior to transfection. According to the protocols of the manufacturer, cells were transfected using Lipofectamine 2000 reagent (Invitrogen, CA). Control cells were only transfected with the Lipofectamine 2000 reagent.

GFP-Fused FAK Constructs and Transfection of Cells

FAK-NT1 (a.a. 1–126), FAK-NT2 (a.a. 127–243), and FAK-NT3 (a.a. 244–415) were amplified by PCR using gene specific primers and cloned into the pEGFP-C2 vector (Clonetech, Mountain View, CA). All sequences were confirmed by automatic sequencing (ICBR Sequencing Facility, University of Florida). To over-express FAK fragments, plasmids pEGFP-

FAK-NT1, pEGFP-FAK-NT2 and pEGFP-FAK-NT3 were transfected into cells with Lipofectamine 2000 (Invitrogen, CA) according to instructions from the provider.

Stable Transduction of Cell Lines

Infection of pancreatic cancer cell lines, Panc-1 and Mia paca-2 was done in the laboratory of Dr. Lung-ji Chang. The lentiviral vectors for luciferase expression were registered on RD-0637 and RD-0633 protocol at the University of Florida.

Pancreatic cancer cell lines were trypsinized and counted. The cells were then plated to 24-well trays and incubated at 37°C, humidified 5%CO2-95% air until 60-80% confluent. In each well, volume of 10 µl the firefly luciferase and red fluorescent protein (RFP) containing lentivirus particles were added to the medium. After gently swirling the plate to mix, cells were incubated at 37°C in a humidified incubator in an atmosphere of 5% CO2, to allow the optimal transduction efficiency. Four hours later, viral containing medium replaced with fresh medium. Based on expression of RFP protein and flow cytometric sorting of the cells, the pure population of transduced cell was obtained.

Detachment Assay

Cells were plated with and without inhibitors for 24, 48, and 72 hours, and detached and attached cells were counted in a hemocytometer. I calculated the percent of detachment by dividing the number of detached cells by the total number of cells. The percent of detached cells was calculated in three independent experiments.

Apoptosis Assays

Tunnel Assay

After treatment of cells for 24, 48, and 72 hours, attached and detached cells were collected, counted and prepared for terminal uridine deoxynucleotidyl transferase (TUNEL) assay by utilizing an APO-BRDU kit (BD Pharmingen, San Diego, CA) according to the

manufacturer's instructions. Stained cells were analyzed with a FACSCalibur cytometer (Becton Dickinson, San Jose, CA). Calculation of the percentage of apoptotic cells in the sample was completed with CellQuest software (BD Biosciences).

Hoechst Staining

In addition, apoptotic cells were also analyzed by Hoechst staining. To the prepared cells as described above, Hoechst 33342 (1 μg/ml) was added, incubated in the dark room temperature for 10 minutes, and the specimens were mounted on glass coverslips. The slides were viewed under the Zeiss microscope for apoptotic nuclei. The percent of apoptotic cells was calculated as the ratio of apoptotic cells to total number of cells. Over 300 cells per sample were analyzed.

Caspase 3/7 Apoptosis Assay

For detection of activated caspase 3/7 enzymes, as a confirmation of apoptosis in the treated cells, Apo-ONE® Caspase-3/7 Reagent kit was used (Promega, Madison, WI). 2000 cells were plated into a 96 well glass bottom plate, and treated with different concentrations of the compound. 24, 48 and 72h after the treatment, cells were incubated with 10 □L of a profluorescent caspase-3/7 consensus substrate, rhodamine 110 bis-(N-CBZ-L-aspartyl-L-glutamyl-L-valyl-aspartic acid amide) (Z-DEVD-R110), for 30 minutes in the dark at room temperature. Upon cleavage on the C-terminal side of the aspartate residue in the DEVD peptide substrate sequence by caspase-3/7 enzymes, the rhodamine 110 becomes fluorescent when excited at a wavelength of 498nm. The emission maximum is 521nm. The amount of fluorescent product generated is representative of the amount of active caspase-3/7 present in the sample. Imaging was with a Leica TCS SP5 laser-scanning confocal microscope with LAS-AF imaging software, using a 40x oil objective.

Kinase Profiler Screening

Kinase specificity screening was performed with Invitrogen's SelectScreen® Kinase Profiling Services http://www.invitrogen.com/site/us/en/home/Products-and-Services/Services/Discovery-Research/SelectScreen-Profiling-Service/SelectScreen-Kinase-Profiling-Service.html. The screening was performed with 1 μM compound, INT2-31, 10μM ATP, and kinase substrates against ten recombinant kinases according to Z'-LYTE™ Kinase Assay. For PI3 kinase activity, 100μM ATP, and kinase substrate were utilized with the Invitrogen Adapta® Universal Kinase Assay protocol.

Tumor Growth in Nude Mice *in vivo*

Six week old athymic, female nude mice were purchased from Harlan Laboratory. The mice were maintained in the animal facility, and all experiments were performed in compliance with NIH animal-use guidelines and under the University of Florida Institutional Animal Care and Use Committees (IACUC) approved protocol.

Melanoma Xenograft

For melanoma study, the University of Florida IACUC approved the following protocol (IACUC Study #200801077). Melanoma cells were injected, 5×10^6 cells, subcutaneously. When the tumor size reached $100mm^3$, the INT2-31 was introduced by intraperitoneal injection at a dose of 15 mg/kg daily. Tumor diameters were measured with calipers, and tumor volume in mm^3 was calculated using the formula $[(width)^2 \times length]/2$. At the end of experiment, tumor weight and volume were determined.

Patient Subjects and Xenograft

The use of human subjects in this study is for the sole purpose of the procurement of solid esophageal and pancreatic tumor tissue for studies reviewed and the specific approval of the

University of Florida Health Center Institution Review Board (IRB) under protocols # 276-2008 and 321-2005 has already been obtained.

For tumor samples from human patients with esophageal or pancreatic cancer, the University of Florida IACUC approved the following protocol (IACUC Study# 2000902767). Up to now, a total of 25 patients, 10 with pancreatic cancer and 15 with esophageal cancer identified and implanted into nude mice. Initially small pieces (0.3 x 0.3 x 0.3 cm) from fresh pancreatic and esophageal human tumor samples were obtained from surgical specimens of patients operated at the University of Florida Shands Hospital, and implanted subcutaneously in-group of 2 mice for each patient. For esophageal cancer specimens, when one of them has reached 1.5 cc, it excised and was cut into small pieces of (0.3 x 0.3 x 0.3 cm), and transplanted subcutaneously into another 10 mice. When tumors reached ~ 100 mm^3, mice were randomized in the following 2 groups, with 5 mice in each group:

- Group 1: Control: no treatment.
- Group 2: INT2-31 (Compound 31): 50 mg/kg/ day in 50 □L by i.p administration for 21 days. This drug has been previously tested by our laboratory and has no measurable toxicity at this dose.

Mice were euthanized 30-40 days after tumor innoculation and tumor and tissue collected. For inhibition of tumor growth in our subcutaneous model, tumor volumes (length X width X height X p/ 6) and body weights were determined daily including weekends and holidays, to monitor tumor growth and evaluate overall clinical condition, taking into account weight loss and indications of pain, distress, or abnormal behavior and physiology. Experiments were terminated when the mean control tumor volume is 1.5cc (approximately 30-40 days).

Antitumor activity was expressed as T/C% (mean increase of tumor volumes of treated animals divided by the mean increase of tumor volumes of control animals multiplied by 100).

Orthotopic model of pancreatic cancer

For othotopic model of pancreatic cancer, the University of Florida IACUC approved the following protocol (IACUC Study# 2000801506). The pancreatic cancer cell lines, Mia paca-2 and Panc-1 cells were stably transfected using luciferase-RFP (red fluorescent protein) reporter gene for *in vivo* imaging of the xenografts. Following expansion and sorting of RFP positive cells, cells were expanded in culture and $5x10^6$ tumor cells were implanted into pancreas of 20 mice. For intra-pancreatic implantation of cells, mice were anesthetized with Isoflurane using the ACS provided and maintained rodent anesthesia machine. Under sterille surgical conditions, via 1.0 cm incision of the skin, abdominal wall and peritonium, the spleen was retracted and cells were injected in 30 L volume into the tail of the pancreas using a 29-gauge needle. The abdominal wall and peritoneum was sutured using 5.0 absorbable surgical sutures and the skin was closed with medical glue (dermabond). Postoperative analgesia was 0.05 mg/kg of buprenorphine subcutaneously per 8-12 hours postoperatively.

When tumors reach ~ 100 mm^3, mice were randomized in the following 4 groups, with 3 mice in each group:

- Group 1: Control: no treatment.
- Group 2: Gemcitabine: 40 mg/kg in 50 μL treated every 5 days for three weeks by intraperitoneal (i.p) administration.
- Group 3: INT2-31: 15 mg/kg/ day in 50 μL by i.p administration
- Group 4: Combination of Gemcitabine and INT2-31 treatments

Mice were hand restrained prior to intraperitoneal injections. Mice were euthanized 6 weeks after tumor innoculation and tumor and tissue collected. As described below, mice were

imaged weekly with the IVIS lumina imager and tumor size will be estimated by the bioluminescent signal.

In vivo Imaging of Mice

I performed noninvasive imaging in all tumor-bearing mice expressing bioluminescent tags. I used the IVIS lumina platform and employed tumors that express a luciferase reporter gene. To accomplish the imaging, mice were anesthetized with Isoflurane using the ACS provided and maintained rodent anesthesia machine. I used a cryogenically cooled IVIS Imaging System (Xenogen) with Living Image acquisition and analysis software (Version 2.11, Xenogen) to detect the bioluminescence signals in mice. For mice bearing tumors expressing a luciferase reporter gene, prior to imaging, mice were injected intraperitoneally or subcutaneously with 150 mg of luciferin (Xenogen Corp., Alameda, Calif.) per kg of body weight in 100 μL using a 25-27 g needle. The area of injection was cleaned using standard surgical disinfectant, all solutions are sterile and satisfy the drug policy of the University of Florida. After 10 min, the mice were anesthetized as described above and placed on heated sample shelf. The imaging system first took a photographic image in the chamber under dim illumination; this followed by luminescent image acquisition. An integration time of 1 min will be used for luminescent image acquisition for all mouse tumor models. I used Living Image software to integrate the total bioluminescence signals (in terms of photon counts) obtained from mice. The *in vitro* detection limit of the IVIS Imaging System is 1,000 ES-2/luc cells.

Each animal studied no more than weekly over a six weeks period. Based on the luminescent signal, the tumor size can be easily estimated. On day 42 or when the tumor size reached 1.5 cc in size, the mice were euthanized.

Immunohistochemistry

Xenograft tumor tissue was fixed in 10% formalin and embedded in paraffin. For Ki67 staining, samples underwent deparaffinization utilizing 3% hydrogen peroxide and blocked with methanol for 10 minutes. Antigen retrieval was performed with pH 6 Dako solution (s1699) heated in a steamer for 20 minutes followed by a 20 minute cool down in solution. Following antigen retrieval, the samples were incubated with the blocking reagent, Background Sniper (BioCare), for 15 minutes. Subsequently, the primary antibody, Ki-67 (Dako M7240), was applied at 1:200 concentration and incubated overnight at 4^{o}C. The secondary antibody used was Mach 2 Anti-Mouse HRP Polymer (BioCare), applied for 30 minutes. The tissues were stained with the chromogen DAB and counterstained with hematoxylin and 1% TBS.

For assessment of apoptotic cells, in situ TUNEL staining (DeadEnd^{TM} Colorimetric Apoptosis Detection System, Promega, Madison, WI) was performed according to instructions from the provider.

Statistical Analyses

Data presented are the means and 95% confidence intervals of the three or more experiments. For *in vitro* and *in vivo* experiments comparison between groups were made using a two-tailed two-sample Student's t test. Differences for which P value was less than 0.05 were considered statistically significant.

Further Studies

Up to present, I have been evaluating a couple of lead compounds that target the interaction site of FAK and IGF-1R. Currently, I have started to evaluate derivatives of our leading compounds to modify their structures to achieve optimal target binding. In addition, characterization of the structural features of the compounds would allow us to define a site on the compound where I can place a ligand to bind our compound to a column and capture proteins

from cell lysates to determine possible interaction partners of the compound. To test the binding of derivatives of the compounds and their ability to disrupt protein-protein interactions we are planning to use ELISA and Biacore analysis as biophysical approaches.

ELISA Test

Two different enzyme-linked immunosorbent assays were performed to study binding between IGF-1R beta subunit and FAK-NT. The first assay involves interaction of IGF-1R with immobilized FAK-NT; the second involves interaction of FAK-NT with immobilized IGF-1R.

In the first case, 96-microtiter plate wells were coated with purified GST-fused FERM domain of FAK in 50 µl of PBS (NaCl 137 mM, KCl 2.7 mM, Na_2HPO_4 4.3 mM, KH_2PO_4 1.4 mM) overnight at 4°C. Wells were then rinsed with wash buffer (PBS, 0.05% Tween) and blocked with 200 µl of blocking buffer (PBS, 1% BSA) for 3 h at 37°C. After rinsing three times with wash buffer, with or without the compounds,100 µl of binding buffer (PBS, 0.05% Tween, 1% BSA) containing 0.2 µM of purified IGF-1R whole protein was added to the wells and let to react for 1 h at 37°C. Wells were rinsed again three times and 100 µl of binding buffer containing 200 ng/ml of a primary antibody anti-IGF-1R (sc-613 Santa Cruz) was added and incubated for 1 h at 37°C. After three additional rinsings, 100 µl of the same buffer containing a secondary HRP anti-rabbit antibody was added and incubated for another hour at 37°C. Finally, 100 µl of ABTS substrate (2,2'-azinobis [3-ethylbenzothiazoline-6-sulfonic acid]-diammonium salt) was applied and the plate was kept in the dark until the color intensity of positive controls was maximum and the negative controls did not develop nonspecific reactions (6–10 min). The ELISA plate was scanned in a Biotech ELISA reader at 450 nm.

For the second assay, the same method was applied, but IGF-1R was immobilized in the wells and incubated with FAK-NT. Primary antibody anti-FAK-4.47 (05-537, Upstate) was used to reveal the binding reaction.

BIACORE Analysis

Biacore T100 technology was used in conjunction with ELISA analysis to characterize the thermodynamic binding parameters of small-molecule compounds targeting interaction site of FAK and IGF-1R.

All experiments were performed using a Biacore T100 optical biosensor (http://www.biacore.com). Series S CM5 sensor chips, N-hydroxysuccinimide (NHS), N-ethyl-N′-(3-dimethylaminopropyl) carbodiimide (EDC), ethanolamine HCl, and instrument-specific consumables and accessories were provided by ICBR at the University of Florida.

FAK-NT immobilization

In order to reuse of sensor chip for both FAK and IGF-1R, I decided to immobilize anti-mouse secondary antibody to the sensor chip surface. By this way, I would be able to use primary antibody to immobilize the ligand protein on the surface as well as eliminating the possibility to masking the interaction site of proteins during immobilization of protein on the chip surface.

Immobilization procedures were performed using Hepes-buffered saline (HBS: 10 mM Hepes and 150 mM NaCl, pH 7.4) as the running buffer. Sensor chip surfaces were first preconditioned with two 6-s pulses each of 100 mM HCl, 50 mM NaOH, and 0.1% sodium dodecyl sulfate (SDS) at a flow rate of 100 µl/min. Anti-mouse antibody surfaces were prepared using amine-coupling chemistry at 30 °C and at a flow rate of 10 µl/min. NHS/EDC was injected for 15 min to activate the surface, 100 µg/ml antibody (dissolved in 10 mM sodium acetate, pH 4.5) was injected for 10 min, and finally ethanolamine was injected for 7 min to block residual

activated groups. This immobilization procedure yielded 5000 to 7000 resonance units (RU) of immobilized antibody. After immobilization, the instrument was primed extensively with the analysis running buffer (50 mM Tris–HCl, 150 mM NaCl, 10 mM MgCl2, 0.1% Tween 20, 0.1% Brij-35, and 5% dimethyl sulfoxide [DMSO], pH 8.0). After immobilization of anti-mouse antibody, 100 µg/ml mouse-anti-FAK 4.47 antibody (05-537, Upstate) (dissolved in 10 mM sodium acetate, pH 4.5) was injected for 10 min, and sensor chip surfaces were washed to remove unbound antibodies with three 5-s pulses each of 100 mM HCl, 50 mM NaOH, and 0.1% sodium dodecyl sulfate (SDS) at a flow rate of 100 µl/min. This immobilization procedure yielded 15000 to 20000 resonance units (RU) of immobilized primary antibody. Finally, 200 µg/ml FAK-NT (dissolved in 10 mM sodium acetate, pH 4.5) was injected for 10 min and and sensor chip surfaces were washed with three 5-s pulses each of 100 mM HCl, 50 mM NaOH, and 0.1% sodium dodecyl sulfate (SDS) at a flow rate of 100 µl/min. This immobilization yielded 30000 to 40000 resonance units (RU) of immobilized FAK-NT.

Capture of IGF-1R

Aliquots of IGF-1R were kept frozen at −80 °C until use. A volume of freshly prepared, 200 µg/ml IGF-1R (dissolved in 10 mM sodium acetate, pH 4.5) was injected for 10 min and unbound protein was removed by passing the solution over a fast desalting column (equilibrated with 50 mM Tris–HCl, 150 mM NaCl, and 10 mM MgCl2, pH 8.0) twice. The capture procedure yielded typically to densities of 2000–4000 RU) onto a FAK-NT surface at 25 °C. A primary antibody bound surface served as the reference.

Preparation of analyte solutions

For stock solutions, the compounds were dissolved in 100% DMSO to a concentration of 10 mM; further dilutions of the compound stocks into DMSO and/or running buffer were performed immediately prior to analysis. To match precisely the DMSO content of the analytes

and running buffer, a secondary stock of lower concentration was prepared by diluting the compound in DMSO to a concentration such that the addition of 50 µl of this secondary stock to 1 ml of 50 mM Tris–HCl, 150 mM NaCl, 10 mM MgCl2, 0.1% Tween 20, and 0.1% Brij-35 (pH 8.0) yielded a compound concentration that was nine times greater than the high concentration chosen for analysis. This starting concentration was diluted ninefold in analysis running buffer to yield the high concentration. An additional ninefold dilution of this sample produced the low concentration. The propagated errors in the concentrations of the high and low analyte concentrations were calculated to be approximately 3.0%.

Analysis parameters

At each temperature, five buffer blanks were first injected to equilibrate the instrument fully. Using a flow rate of 50 µl/min, compounds were injected for 30 to 60 s and dissociation was monitored for 1 to 20 min. (The selected injection and dissociation times were determined in preliminary binding tests.) For the tightly bound complexes, a regeneration step was required. At 4 to 11 °C, the surface was regenerated with 10 100-s pulses of 60% ethylene glycol; at 16 to 18 °C, 40% ethylene glycol; at 22 to 28 °C, 30% ethylene glycol; and at 32 to 39 °C, 50 mM Tris–HCl, 150 mM NaCl, 10% ethylene glycol, 15 mM ATP, 15 mM MgCl2, 5% DMSO, and 0.1% Tween 20 (pH 8.0). The data collection rate was 10 Hz.

Data analysis

Biosensor data, processed and analyzed using Scrubber 2 (BioLogic Software, Australia), were fit to either a simple 1:1 model (A + B = AB) or a 1:1 interaction model that included a mass transport term (Ao = A, A + B = AB). Equilibrium dissociation constants determined in Scrubber were fit to the van't Hoff equation $\ln(KD) = \Delta H°/RT - \Delta S°/R$. (Although the use of integrated forms van't Hoff equation that includes a term for $\Delta Cp°$ was considered, the lack of curvature in the ln(KD) versus 1/T plots indicated that using this approach was unnecessary.)

Values for ΔH° and ΔS° were obtained directly using the Solver macro in Microsoft Excel. ΔH° and ΔS° values were also determined indirectly via linear regression analysis of ln(KD) versus 1/T plots using the Regression function in Excel, where the slope and intercept corresponded to ΔH°/R and−ΔS°/R, respectively. Fitting errors for ΔH° and ΔS° from Solver were obtained using a downloadable macro called SolverAid (http://www.bowdoin.edu/~rdelevie/excellaneous). Errors for the parameters ΔH° and ΔS° from the Regression routine were obtained directly from a statistical readout in Microsoft Excel. The values obtained from both methods agreed well. Standard errors were propagated according to the general formula $\Delta z2=(\partial f/\partial x)2\Delta x2+(\partial f/\partial y)2\Delta y2+\ldots$ in Excel. Programmed formulas were first checked using the downloadable macro Propagate (also available at http://www.bowdoin.edu/~rdelevie/excellaneous).

CHAPTER 3
RESULTS AND DISCUSSION

Results

Structure-Based *in silico* Molecular Modeling and Computational Docking

Previous studies in our laboratory have demonstrated that the amino terminus of FAK (aa 127-243, FAK-NT2) directly binds with a portion of the intracytoplasmic portion of IGF-1R, containing kinase domain (aa 959-1266) (Zheng et al.2009). In collaboration with Dr. David Ostrov, we analyzed the possible models of interaction of the FAK FERM domain and IGF-1R kinase domain using DOCK5.1 computer program and selected small molecule compounds predicted to disrupt these proteins interactions. Based on the known crystal structures of the FAK FERM domain and IGF-1R kinase domain, the pmol computer program predicted three possible orientations for the interaction (Figure 3-1). 250,000 small-molecule compounds from NCI Database with known 3D structure and which correspond to Lipinski rules were docked into the site of interaction between FAK and IGF-1R in 100 different orientations for each possible orientation. The top scoring compounds were obtained from the National Cancer Institute Developmental Therapeutics Program. The initial screening of IGF-1R/FAK targeted small molecules was performed based on compounds effect on cell viability using MTT assay (Figure 3-2). Subsequently, compounds with high probability to bind to the interface (by predicted energies of interaction) and causing reduced cell viability were screened for their ability to inhibit the interaction of FAK and IGF-1R. Among all the compounds tested, I identified our lead compound, INT2-31 (NSC 344553), as the most potent FAK/IGF-1R binding inhibitor (Figure 3-3). This compound is listed as interacting in the third predicted orientation of FAK with IGF-1R (Table 3-1). The structure and predicted energies of interaction are demonstrated in Figure 3-4. The intermolecular energies for all configurations of INT2-31 in binding to FAK-NT

were calculated as the sum of electrostatic and van der Waals energies. These energy terms were evaluated as correlation functions, which were computed efficiently with Fast Fourier Transforms.

INT2-31 Disrupts the Interaction of FAK and IGF-1R

The potency of INT2-31 to disrupt the protein-protein interactions of FAK and IGF-1R was evaluated by pull down assays using tagged purified protein constructs. INT2-31 caused a dose dependent decrease in binding between purified GST-FAK-NT and IGF-1Rβ with an average IC_{50} of 3.96 μM (Figure 3-5). Because other compounds had higher predicted energies of interaction with the FAK-FERM domain as compared to INT2-31, I evaluated several top scoring compounds for their effects on the disruption of the interaction between FAK and IGF-1R. I chose to evaluate compounds that both inhibited cell viability by MTT and those that did not significantly reduce cell viability. It is possible that compounds that did not reduce cell viability were not able to penetrate into the cell and therefore, required testing in purified protein assays using GST pulldowns. If compounds could disrupt protein interactions but not reduce cell viability, such compounds could be considered for modifications allowing for better cell penetration. Therefore, two other high scoring compounds that demonstrated affinity for the FAK-FERM domain, but did not significantly alter cell viability by MTT assay were evaluated and were found to not disrupt the binding by GST-pulldown.

To characterize effects of INT2-31 *in vitro* I chose two melanoma cell lines that we already had in our lab and first analyzed FAK and IGF-1R expression. I found that INT2-31 disrupted binding in C8161 and A375 melanoma cancer cells at low micromolar concentrations (IC_{50} of 2.72 and 3.17 μM, respectively) as demonstrated by co-immunoprecipitation assay (Figure 3-6-A, B). In contrast, another NCI compound (NSC 250435, “compound 17”) that was shown to

inhibit cell viability by MTT assay, did not disrupt the protein interaction by co-IP in C8161 cells.

INT2-31 Reduces the Viability of Cancer Cells

To determine the effect on melanoma cell viability, three human melanoma cell lines were exposed to increasing doses of INT2-31 over 72 hours and the results compared to human melanocytes. As shown in Figure 3-7, INT2-31 inhibits viability of cancer cells more than normal cells. All three melanoma cell lines had upregulated FAK and IGF-1R expression and increased sensitivity to INT2-31 compared to normal human melanocytes. The effects of INT2-31 varied in the three cell lines and were possibly related to constitutive FAK and IGF-1R activation with the least sensitive cell line (SK-MEL-28) having the greatest expression of FAK and IGF-1R.

In addition, I analyzed the effect of INT2-31 on cell viability of esophageal, pancreatic and breast cancer cell lines and determined the IC_{50} value for each cell lines as shown in Table 3-2. To get the average IC_{50} value, each cell line was treated with increasing concentrations of the compound for 72 hours in triplicates and the average of IC_{50} values from three separate experiments was calculated. Similar to melanoma results, INT2-31 inhibits viability more in cancer cells compared to normal cells. Of note, sensitivity of the cells to INT2-31 varies and directly correlated to FAK and IGF-1R expression in the cells.

INT2-31 Inhibits Cancer Cell Proliferation and its Activity Depends on the Presence of FAK and IGF-1R

To assess the effects of INT2-31 on cell proliferation, a CSFE cell distribution assay was performed. As shown in Figure 3-8, INT2-31 inhibited cell proliferation in both C8161 and A375 cells with C8161 cells being more sensitive. A time course of cell counting demonstrated potent inhibition of the growth of C8161 melanoma cells (Figure 3-9). After 24 hours of

treatment, cell number was decreased by more than 60%, which correlates with MTT data (Figure 3-7). I also obtained similar results when I analyzed the effects of INT2-31 on cell proliferation in esophageal and pancreatic cancer cell lines (data not shown).

To show that the effect of INT2-31 was specific for cells expressing FAK, C8161 were treated with FAK shRNA constructs resulting in transient knockdown of FAK (Figure 3-10-A). C8161 cells expressing FAK shRNA were significantly less sensitive to the effects of INT2-31 than parental and mock transfected cells (Figure 3-10-B). Currently, I are designing shRNA constructs to stably knockdown of FAK in esophageal and pancreatic cell lines to perform *in vitro* and *in vivo* experiments to show the specificity of the compound.

Moreover, I assessed the specificity of compound on FAK and IGF-1R proficient and deficient mouse embryonic fibroblasts (MEFs). The treatment of cells with 0.01 to 1 μM concentrations of INT2-31 for 72 hours was analyzed by MTT assay. As shown in Figure 3-11-A, B, FAK-/- and IGF-1R -/- fibroblasts were significantly less sensitive to the effects of INT2-31 than FAK+/+ and IGF-1R +/+ cells ($p<0.05$). On the other hand, the dual inhibitor of FAK and IGF-1R, TAE 226 (Novartis, Basel) control was ineffective on IGF-1R -/- yet reduced the viability of FAK-/- cells (Figure 3-11). The sensitivity of FAK-/- cells to TAE 226 is very likely due to nonspecific effects of TAE 226 with inhibition of IGF-1R kinase activity and possibly other kinases.

INT2-31 Induces Apoptosis but not Detachment

Since FAK is an important protein for adherence of cells and targeting FAK raises concern about the detachment and metastasis of cancer cells, I assessed the effect of INT2-31 on detachment of treated cells. Detachment of cells was determined in the presence of increasing concentrations of INT2-31. As shown in Figure 3-11, only 7% of C8161 cells detached from the plate after 72 hours of treatment with 5μM of INT2-31. The effect of INT2-31 was significantly

less than the dual FAK and IGF-1R kinase inhibitor, TAE 226 (Novartis, Basel). This result shows that inhibition of the kinase activity of FAK may allow cancer cells to become detached and metastasize, whereas disruption of interaction between FAK and IGF-1R with a small molecule blocks downstream signaling without interfering normal function of FAK. Similar to melanoma cell lines, adherence of esophageal and pancreatic cancer cell lines were unaffected by the treatment of compound (data not shown).

The effect of INT2-31 on cell survival was marked with a greater than 50% induction of cell death as indicated by the detection of apoptotic cells in Hoescht staining after 72 hours of treatment with a 5 μM dose (Figure 3-13). This was confirmed by presence of activated caspase 3/7 in C8161 melanoma cells after treatment for 48h with 1 μ M and 5 μ M of INT2-31 as detected by confocal microscopy (Figure 3-14). Finally, the effect of INT2-31 was evaluated by Western blot. As demonstrated in Figure 3-15, PARP and caspase-9 cleavage is seen after 48 hours treatment with INT2-31 at low 1 μM concentration. There was no significant effect of INT2-31 on caspase 8 levels indicating induction of apoptosis through activation of the intrinsic pathway only.

INT2-31 Decreases Activation of Akt

The effect of INT2-31 on FAK and IGF-1R pathway effectors was analyzed in three melanoma cell lines at different concentration and treatment times (Figure 3-16). INT2-31 treatment resulted in a consistent inhibition of constitutive and IGF-1 induced signaling to AKT. Of note, there was no significant effect of INT2-31 on the constitutive phosphorylation of FAK or the constitutive or IGF-1induced phosphorylation of IGF-1R. In addition, while there was a pronounced effect on Akt, the effects on signaling to ERK was minimal with a slight decrease in p-ERK in all cell lines after treatment with higher doses. The effects of INT2-31 on p-Akt correlated with the effects on cell growth, viability and apoptosis in melanoma cell lines. C8161

cells were the most sensitive with significant inhibition of p-Akt at 0.5-1 µM, while higher doses of INT2-31 were necessary to significantly decrease p-Akt in A375 and SK-MEL-28 cells (1-5 µM and 5-10 µM, respectively) (Figure 3-16-B, C). The analysis of time course of the INT2-31 treatment on Akt phosphorylation revealed some dephosphorylation after 24 hours of treatment with a sustained effect at 72 hours (Figure 3-16-D). Therefore, INT2-31 decreases signaling through pathways downstream of FAK and IGF-1R.

Because treatment of cells with INT2-31 decreases the phosphorylation of Akt, I evaluated the effect of INT2-31 on kinase activity of proteins that are involved in this signaling pathway. To insure that the decrease in the phosphorylation of Akt is due to disruption of FAK and IGF-1R interaction but not due to off target inhibition of kinases, I utilized the Invitrogen's kinase screening service. The effect of this compound on the kinase activity of FAK, IGF-1R, insulin receptor, VEGFR-1, AKT-1, EGFR, VEGFR-2, c-MET, PDGFRa, p70S6K, Src and PI3Kinase was determined (Figure 3-17). At a dose of 1 µM, this compound did not inhibit the kinase activity of FAK or IGF-1R and did not inhibit any of the other protein kinases by more than 22%.

Furthermore, to confirm that INT2-31 specifically binds to NT2 (aa 127-243) region of FAK to disrupt interaction with IGF-1R and decreases phosphorylation of Akt, I transfected C8161 cells with 3 GFP fragments of the FAK N-terminus (FAK-NT1, FAK-NT2 and FAK-NT3). As shown in Figure 3-18, overexpression of FAK-NT2 fragment reduced the IGF-1 induced phosphorylation of AKT compared to FAK-NT1 and NT3 overexpressed cells. Therefore, it appears that over-expression of the FAK interaction module (FERM-NT2 region) yield the same phenotype. Confirmation of these results is required as FAK overexpression frequently results in cell toxicity and inconsistent results. In addition, FAK-NT fragments

frequently are seen in the nucleus following overexpression and therefore may not accurately reflect findings compared to normal intact FAK expression.

INT2-31 Sensitized Cancer Cells to Chemotherapy

To evaluate and correlate the effect of INT2-31 on Akt de-phosphorylation with the sensitivity of cells to conventional chemotherapy, esophageal and pancreatic cancer cell lines were analyzed for the effects of combination therapies on cell viability and apoptosis. Both KYSE 70 and 140 esophageal cancer cells were sensitive to INT2-31 and 5-FU treatment and 0.5 and 1 μM INT2-31 had synergistic effects with 5-FU (Figure 3-19). In our pancreatic cancer cells, while the effect on cell viability of INT2-31 was only additive when combined with gemcitabine (data not shown), INT2-31 had synergistic effects with 5-FU chemotherapy at 1μM concentrations (Figure 3-20).

INT2-31 Decreases Tumor Growth in Melanoma Xenograft Model Through Inhibiting Phosphorilation of Akt

The effect of INT2-31 was evaluated in two melanoma subcutaneous xenograft models. For defining the optimal dose, I used 100, 50, 20 and 15 mg/kg doses via intraperitoneal injection. The 100mg/kg dose was highly toxic and in a week caused death of two mice out of five (data not shown). The 50mg/kg dose when administrated via daily intraperitoneal injection caused slight body weight loss. Therefore, as demonstrated in Figure 3-21-A and B, I preferred to use the 15mg/kg dose for further experiments. Daily intraperitoneal injection of 15mg/kg of INT2-31 for 21 days resulted in a significant decrease in C8161 and A375 tumor growth compared to mice receiving PBS control injections ($p<0.05$). At this concentration, the drug did not have serious toxicity as there was no significant difference in body weights between animals in each group. To assess the *in vivo* effects of INT2-31 on cell proliferation, I stained C8161 xenografts with Ki67 antibody. As shown in Figure 3-21-C, immunohistochemical staining of

C8161 tumors demonstrated that the percent of cells reactive to Ki67 and the intensity of Ki67 staining were significantly decreased in the C8161 tumors from mice treated with INT2-31 compared to PBS group. In addition, the percent of cells undergoing apoptosis was significantly increased in the tumors treated with INT2-31 compared to control (Figure 3-21-C, $p<0.05$). This confirmed our *in vitro* data that the drug decreases proliferation and increases apoptosis of cancer cells. The effect of INT2-31 on the *in vivo* interaction of FAK and IGF-1R in C8161 tumors was analyzed by immunoprecipitation of FAK from treated and untreated tumor and is illustrated in Figure 3-21-D. Western blot for IGF-1R demonstrates a decrease in the coimmunoprecipitation of FAK and IGF-1R. Densitometry of the ratio of IGF-1R to FAK in each tumor showed a decreased mean ratio in INT2-31 treated (0.78 ± 0.16) compared to PBS treated (0.98 ± 0.11, $p=0.09$) tumor samples. Finally, tumor analysis for p-AKT expression by Western blot analysis demonstrates a decrease in phosphorylation of AKT in animals treated with INT2-31 vs PBS control (Figure 3-21-E). Therefore, our lead compound, INT2-31, decreases *in vivo* tumor growth, disrupts the *in vivo* interaction of FAK and IGF-1R and results in a decrease in phosphorylation of AKT.

In vitro and *in vivo* Inhibition of Esophageal Cancer Viability and Proliferation With INT2-31 Treatment

Esophageal cancer has been shown to overexpress FAK and IGF-1R. To assimilate the effects of targeting the interaction of these proteins in direct patient specimens, I developed a system in which I grow direct esophageal cancer specimens in mice and tissue culture plates to allow fresh human tissue for experimentation. Up to now, I have collected more than 20 tumors and corresponding normal tissue specimens from cancer patients. Immunohistochemical and western blot analysis of the samples also demonstrated increased level of FAK and IGF-1R in tumor samples compared to the normal tissue. To evaluate the *in vitro* effects of INT2-31 on

patient specimens, I utilized MTT assay of cells grown in a tissue culture plate maximum up to eight passages. A representative result of MTT assay of esophageal patient # 5 shown in Figure 3-22-A. Increasing concentrations of INT1-31 effectively decreased the viability of cells with an average IC_{50} value of 2.18 μ M.

Subsequently, I evaluated the inhibition of *in vivo* tumor growth of esophageal patient #5 specimen. As described in methods section, I initially implanted small pieces (0.3 x 0.3 x 0.3 cm) from a fresh esophageal human adenocarcinoma tumor sample subcutaneously into2 mice. When one of tumors has reached 1.5 cc^3, it was excised and cut into small pieces of (0.3 x 0.3 x 0.3 cm), and transplanted subcutaneously into another 10 mice. When tumors reached ~ 100 mm^3, mice were randomized in the 2 groups, with 5 mice in each group. As demonstrated in Figure 3-22-B, daily intraperitoneal injection of 50 mg/kg of INT2-31 for 21 days resulted in a significant decrease in fresh esophageal adenocarcinoma tumor growth compared to mice receiving PBS control injections ($p<0.05$). At this concentration, the drug did not have serious toxic effects, as there was no significant difference in body weights between animals in each group. To assess the *in vivo* effects of INT2-31 on cell proliferation, I stained esophageal patient #5 tumor specimen xenografts with Ki67 antibody. As shown in Figure 3-22-C, immunohistochemical staining of tumors demonstrated that the percent of cells reactive to Ki67 were significantly decreased in the tumors from mice treated with INT2-31 compared to PBS group. This confirmed our *in vitro* data that the drug decreases proliferation of cancer cells and *in vivo* data for melanoma model.

Inhibition of Orthotopic Pancreatic Xenografts With INT2-31 Treatment

Since human pancreatic cancer is an aggressive malignancy with redundant survival pathways, I hypothesized that FAK and IGF-1R physically interact to provide essential survival signals for pancreatic cancer cells. In addition, I hypothesize that simultaneous inhibition of

these signals will induce cellular apoptosis and sensitize these cells to proapoptotic therapies. To further validate the activity and specificity of INT2-31, I employed orthotopic mouse models. The pancreatic cancer cell lines, Mia paca-2 and Panc-1 cells were stably transfected using luciferase-RFP (red fluorescent protein) reporter gene for *in vivo* imaging of the xenografts. Following expansion and sorting of RFP positive cells, cells were expanded in culture and $5x10^6$ tumor cells were implanted into the pancreas of 14 mice. As described in the materials and methods section, mice were imaged weekly with the IVIS lumina imager and tumor size were be estimated by the bioluminescent signal. When tumors reach ~ 100 mm^3, mice were randomized in the following 2 groups, with 7 mice in each group: Control and 15mg/kg INT2-31. As shown in Figure 3-23, daily intraperitoneal 50mg/kg treatment of Miapaca2 and subcutaneous 15mg/kg injection of INT2-31 for 21 days sufficiently reduced the growth of the orthotopic pancreatic xenografts without any significant side effects as measured by body weights and the appearances of the animals.

Discussion

FAK and IGF-1R are two important tyrosine kinases that control many signals leading to proliferation, invasion and metastasis. Our hypothesis is that FAK interacts with IGF-1R to provide essential survival signals for many cancer cells. FAK and IGF-1R also interact with many other proteins that provide survival signals to tumors. The best-defined pathway by which IGF-1R signaling can prevent apoptosis is mediated by phosphoinositide 3-kinase (PI3K) signaling to Akt. Activated Akt/PKB plays a key role in the prevention of apoptosis. It phosphorylates and inactivates several proteins that are involved in apoptosis including Bad (Bcl-2 family member). There is evidence of Akt involvement in human malignancies. Akt was found to be amplified 20-fold in primary gastric adenocarcinoma. Additional

studies have shown genomic amplification and overexpression of Akt in several cancer cell lines (Staal et al. 1987, Ruggeri et al. 1998).

It has been shown that FAK activates proliferation and inhibits apoptosis through PKC and the PI3K-Akt pathway, which results in induction of cyclin D3 expression and CDK activity (Yamamoto et al. 2003). Therefore, activation of either FAK or IGF-1R induces the PI3K-Akt pathway and cell survival. Clearly, there is crosstalk and redundancy in the signaling via these tyrosine kinases, but the pathways diverge as well. Induction of the IGF-1R results in MAPK pathway activation, which is independent of FAK phosphorylation and activation (Albert-Engels et al. 1999). It has been shown that a member of the MAPK pathway (MEK kinase 1) binds to FAK, linking FAK to possible activation of this pathway (Yujiri et al. 2002). It has also been shown that FAK is activated by IGF-1R, and that IRS-1 is a substrate for FAK and that FAK activity regulates IRS-1 mRNA levels (Baron et al. 1998, Lebrun et al. 1998). Furthermore, it has been shown that FAK participates in integrin-mediated phosphorylation of the insulin receptor (Annabi et al. 2001). However, IGF-1R activity is not required for the phosphorylation of FAK and FAK activity is not required for phosphorylation of the IGF-1R. Due to this overlap and divergence in signaling from these tyrosine kinases, inhibition of either pathway alone may not be as efficacious as dual inhibition of both FAK and IGF-1R.

While emerging data strongly suggests that FAK is an excellent target for developmental therapeutics of cancer, specific small molecule kinase inhibitors of FAK have been difficult to obtain (McLean et al. 2005, Van Nimwegen et al. 2007). Three such kinase inhibitors were reported from Novartis (NVP-TAE 226) and Pfizer (PF-573,228 and PF-562,271), but only PF-562,271 is in clinical trials in cancer patients (Shi et al. 2007, Slack-Davis et al. 2007, Roberts et

al. 2008). Industry leaders are exploring the utility of antibodies to the extracellular domain of IGF-1R. These antibodies are under investigation in multiple tumor types. Six companies are currently testing small molecule kinase inhibitors targeting the IGF-1R tyrosine kinase (Pollak et al. 2008, Hewis et al. 2009). Such approaches targeting the ATP competitive binding site lack specificity for IGF-1R or FAK inhibition. Due to sequence homogeneity, particularly in the kinase domain, and structural similarity of IGF-1R to other receptors such as the insulin receptor, the main problem with kinase inhibitors is their lack of specificity. In addition, it frequently appears that disruption of the kinase domain does not specifically interfere with the downstream signaling of FAK or IGF-1R and it is unclear whether the kinase function or the scaffolding function of these proteins is more important.

To date, the approaches to dual FAK and IGF-1R inhibition by our laboratory and others have mainly focused on direct kinase inhibition. In this work, I demonstrate a novel approach for therapy in several cancer types by targeting FAK-IGF-1R protein-protein binding. Our data, using computer modeling and functional approaches has identified a novel small molecule (INT2-31, NSC 344553) that disrupts the interaction of FAK with IGF-1R. This small molecule inhibits FAK and IGF-1R dependent signaling and cancer cell viability *in vitro* and inhibits *in vivo* tumor growth.

It is possible that the observed effects of INT2-31 are due to multiple effects on cancer cells including inhibition of cell proliferation resulting in cell apoptosis. Lending support to this consideration is the structure of INT2-31 as it resembles a nucleoside analog which can have effects on DNA and the cell cycle. Further studies to confirm the mechanism of action of this compound are necessary. In order to confirm that this inhibitor is truly binding to FAK, secondary confirmatory experiments must be undertaken using biophysical techniques. The

molecular mode of action of the FAK-IGF-1R inhibitors at the atomic level, can be provided by co-crystallization with the N-terminal domain of FAK. This will also provide key structural information that will be essential for the rational development of improved compounds. The prospect for novel inhibitors of protein interactions is very promising, especially, when the X-ray crystal structure of the small molecule bound to its target can be obtained. This provides detailed molecular information about the target-small molecule fragment interaction surface on which to build, using in silico methods, chemicals that both look like the binding site and have similar contacts with the target molecule. Other non-crystallographic methods such as Biacore and ITC (isothermal calorimetry) should be used to provide evidence of binding. If these methods are not successful in evaluating the kinetics of interaction of INT2-31 with FAK and/or IGF-1R, alternative approaches are routinely available such as an ELISA assay as a secondary method to validate target interaction. Demonstration of physical binding by these methods is important as a triage step prior to co-crystallization.

Although our data suggests that INT2-31 does not significantly alter the kinase activity of the 12 kinases selected for study, it is still possible that INT2-31 alters the kinase activity of other kinases. Since, a limited kinase profiler screen was performed showing lack of direct target inhibition and it would be worthy to expand this screen to potentially identify some targets that may be regulating cell cycle progression as this (rather than apoptosis) connection is the strongest with regard to connecting the *in vitro* with *in vivo* effects. In addition, while some cell lines are sensitive to INT2-31 inhibition at submicromolar and low micromolar concentrations, others are not and it may be useful to evaluate the effect of 5-25 μM of INT2-31 on the kinase activity of multiple selected kinases.

FAK is a large molecule that interacts with IGF-1R and several other receptor tyrosine kinases including EGFR and VEGFR-3 as well as other cytoplasmic proteins including paxillin and p53. The specificity of our lead compound, INT2-31, to disrupt the interactions of IGF-1R at the amino terminus of FAK (aa 126-243) should be confirmed as compared to other molecules known to interact with FAK at the C terminus. To determine the selectivity of the inhibitors for FAK/IGF-1R binding over FAK binding to other proteins such as paxillin, VEGFR-3 and Src, we will perform similar studies with HA-tagged paxillin, HA-VEGFR-3 and HA-Src and FLAG-tagged FAK. Furthermore, it also possible to determine the selectivity of INT2-31 for FAK/IGF-1R binding over other protein-protein interactions. For example, the ability of INT2-31 to disrupt the binding of HA-Grb2 to FLAG-SOS and HA-p85 (PI3K subunit) to FLAG-EGFR will also be determined using the same whole cell assay.

The rationale for combination cytotoxic therapy is centered on interfering with different biochemical targets, overcoming drug resistance in heterogeneous tumors, and by taking advantage of tumor growth kinetics with increasing the dose-density of combination treatments. The overall goal is to improve clinical efficacy with acceptable toxicity. Our data demonstrates that there may be synergistic activity between INT2-31 and 5-FU but not gemcitabine. Some chemotherapeutic agents are more cell cycle dependent than others. The available data suggests that gemcitabine's activity is cell cycle dependent while 5-FU is not (Allegra et al. 1997). With our increased understanding of the cell cycle and the impact chemotherapeutic agents have on the cell cycle, it is increasingly apparent that this can create drug resistance, thereby reducing combination chemotherapeutic efficacy. This is particularly relevant with the advent of cell cycle-specific inhibitors but also has relevance for the action of standard chemotherapeutic

agents currently in clinical practice. Appropriate sequencing and scheduling of agents in combination with chemotherapy may overcome this cell cycle mediated resistance.

Our studies provide *in vivo* proof of principle that inhibitors of protein–protein interactions can be efficacious anticancer drugs. Previously, this approach has been successfully used to target FAK-VEGFR-3 protein interactions (Kurenova et al. 2009). Therapy could be individualized to melanoma or other malignancies with cancer-related FAK or IGF-1R overexpression. Disruptors of protein-protein interactions may be active without the genotoxicity of traditional cancer chemotherapy or radiation therapy. This lack of genotoxicity may reduce both DNA damage in normal cells and the potential of inducing mutant clones of cancer cells that are resistant to cancer therapy. Successful incorporation of an approach targeting protein-protein interactions would greatly expand the available treatment options for neoplasms, such as metastatic melanomas, that are resistant to all known therapy.

The strategy of using drug-like small molecules to block such protein–protein interactions has not been considered as attractive by both academia and the pharmaceutical industry as are inhibitors of key cancer-related enzymes such as kinases. While enzymes are in principle amenable to blocking by small molecule inhibitors, other therapeutic routes are needed for a large number of cancer targets that work via protein-protein interaction. However, the current dogma argues for the intractability of protein-protein interaction as a small molecule drug target due to the large and often flat surfaces where two proteins bind to each other. Some successes have begun to appear, such as Nutlin-3 specifically binding to MDM2, inhibiting MDM2-p53 interaction and activating p53 and indeed the notion of the intractability of ablating protein interactions is being questioned (Vassilev et al. 2002). Recently, evidence has begun to

accumulate that interference with protein interactions can be a route to design of cancer drugs, including macrodrugs and small molecules.

In summary, a novel small molecule compound that disrupts the protein interaction of FAK and IGF-1R has potent antineoplastic effects in both *in vitro* and *in vivo* models. Further studies, which explore the targeting of protein-protein interactions, are indicated in diverse tumor types.

Table 3-1. The top scoring compounds for the third orientation

NCI Number	Docking Score	NCI Number	Docking Score
18468	-68.126091	243172	-52.02042389
407817	-67.22935486	47091	-51.94153214
128977	-65.1653595	166346	-51.84930801
407819	-64.94876099	17151	-51.84696198
605085	-63.69062424	37053	-51.82419586
243620	-62.32995224	174007	-51.75821686
128977	-62.24939728	42215	-51.72647095
608071	-62.18764496	244047	-51.58001709
250435	-62.17018127	244047	-51.54472351
243620	-61.87368393	147708	-51.51343155
122277	-61.27615356	163994	-51.33721161
21371	-60.72781372	408182	-51.28966904
21371	-60.30609894	113368	-51.1672287
21371	-60.17605591	174007	-51.05070496
243620	-59.90954208	141845	-50.85812378

Table 3-1. Continued

NCI Number	Docking Score	NCI Number	Docking Score
73712	-59.85826492	8447	-50.79795074
243620	-58.77994156	244047	-50.71466446
93369	-58.23083878	36997	-50.6452179
43078	-58.10844421	141845	-50.6200943
133881	-57.29674149	18951	-50.61251068
40837	-56.9882164	147708	-50.49430466
21371	-56.87865067	379390	-50.48746109
408156	-56.48332977	9019	-50.43544769
129465	-55.56538773	244047	-50.42672729
129455	-55.30924606	59711	-50.41436768
129460	-55.09999084	74737	-50.35530853
122277	-54.89561081	37273	-50.29539871
129448	-54.80198288	141842	-50.27738953
129478	-54.74204254	174007	-50.25862885
46475	-54.56863785	45202	-50.21681976
667507	-54.45470428	49485	-50.21675491
627180	-54.1296463	74737	-50.19744873
4907	-54.01021957	37044	-50.17610168
129463	-54.00395966	**344553**	**-50.12093353**
117489	-53.83126831	68045	-49.93840408
408732	-53.79541779	141845	-49.78398895

Table 3-1. Continued

NCI Number	Docking Score	NCI Number	Docking Score
163897	-53.72097015	255125	-49.78347397
127006	-53.65956879	4460	-49.64286041
129464	-53.6010437	72986	-49.60755157
652894	-53.59884262	60156	-49.6008606
13565	-53.49819946	249211	-49.55879974
405849	-53.44078445	404012	-49.47080994
141172	-53.25966644	7561	-49.44004822
627180	-53.1901207	627180	-49.39595795
141842	-53.1071434	147708	-49.38103867
129466	-52.8824234	41357	-49.13315582
46713	-52.75917053	127010	-49.12238312
46713	-52.54545975	243172	-48.99539566
129468	-52.44723892	287499	-48.97979355
129467	-52.25016785	141842	-48.9745903

Table 3-2. IC_{50} of INT2-31 for cancer cell lines

Cell Lines	[INT2-31] μM
Melanoma	
Melonocyte	97.3
A375	2.7
C8161	0.5
SK-MEL-28	22.1
EsophagealCancer	
TE3	5.6
TE7	3.2
TE9	3.6
KYSE70	4.6

Table 3-2. Continued

Cell Lines	[INT2-31] μM
KYSE140	2.5
KYSE180	19.8
Pancreatic Cancer	
HPDE	
Panc-1	6.7
Miapaca-2	4.73
AsPC1	16.9
BxPC3	45.6
Breast Cancer	
MCF10A	100
MCF7	0.03
BT474	2.39

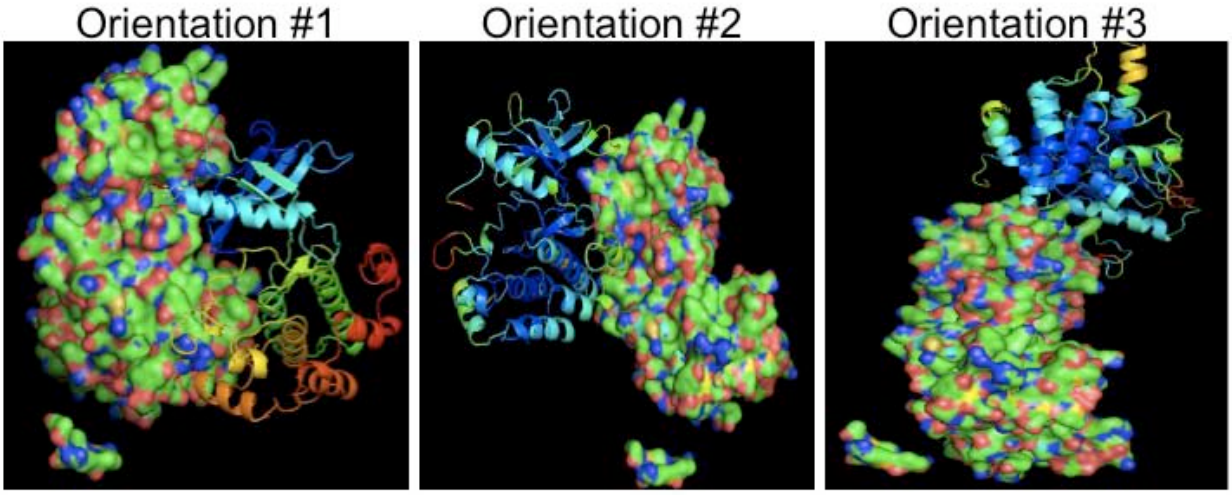

Figure 3-1. Pmol modeling of FAK and IGF-1R interaction based on the known crystal structures of FAK-FERM domain (space filled structure) and IGF-1R ß subunit (shown in helical-ribbon structure). Possible orientation of interaction of FAK and IGF-1R is demonstrated based on computational modeling showing three alternative orientations.

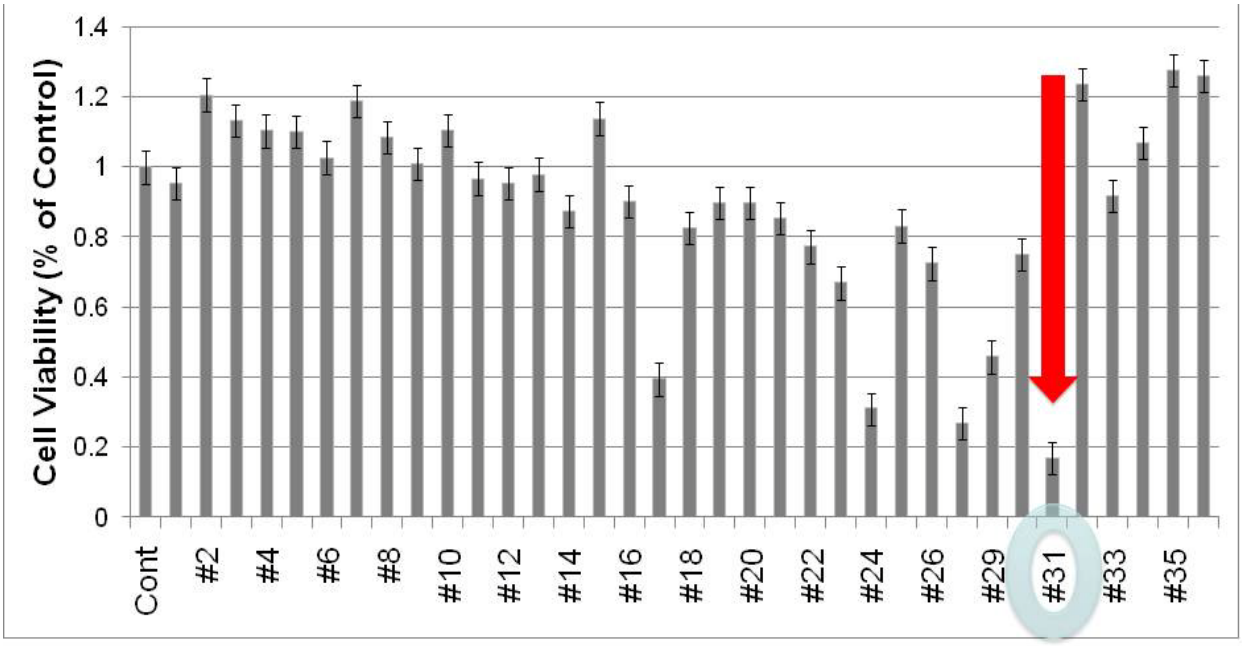

Figure 3-2. Screening of top scoring compounds. MTT assay of compounds with high scores of interaction based on van der Waals and hydrostatic charges. Data shown in Miapaca-2 pancreatic cancer cells at 72 hours with 100µM concentrations of compounds.

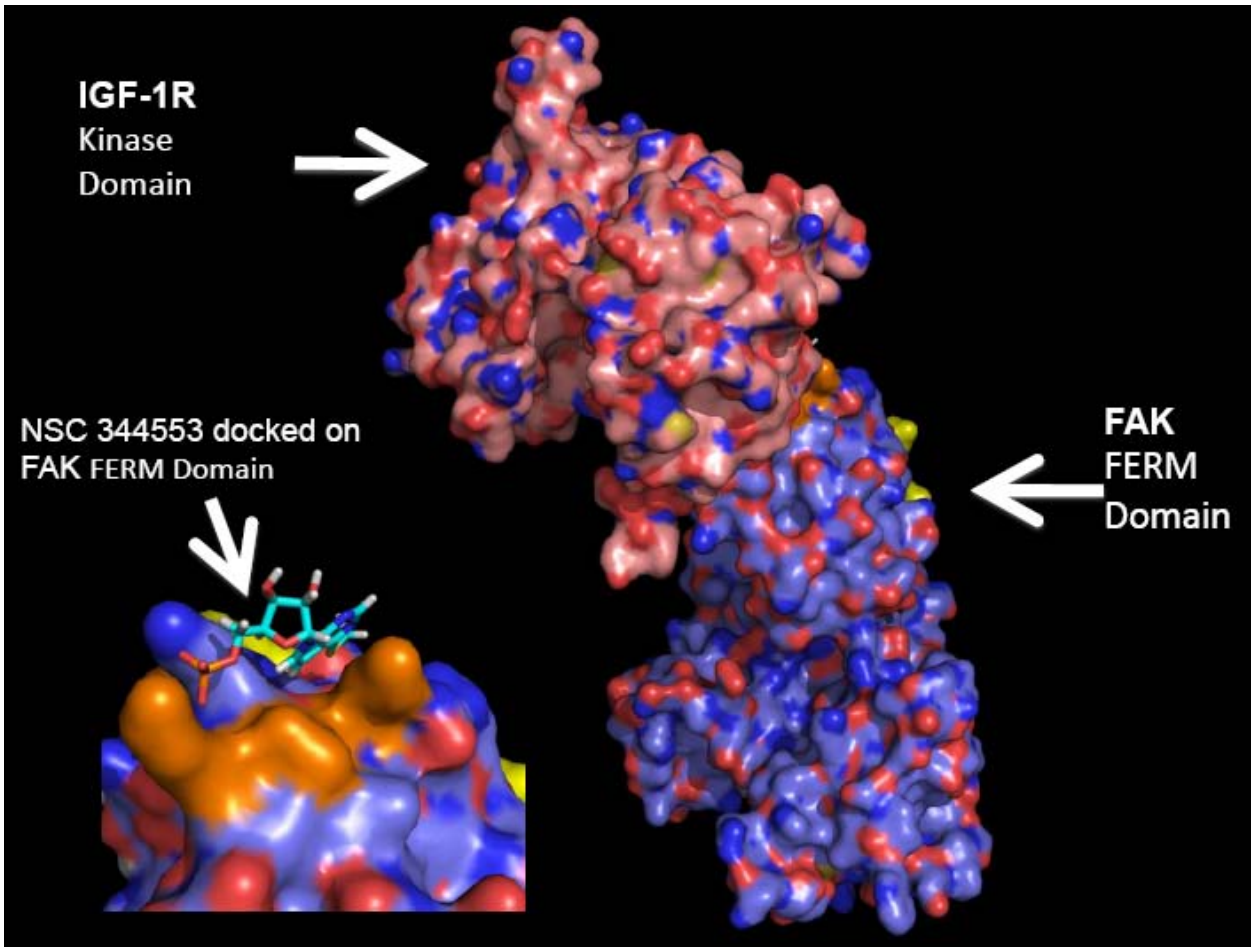

Figure 3-3. In silico modeling of FAK and IGF-1R interaction. The proposed site of interaction of FAK and IGF-1R is demonstrated based on computational modeling. Lead small molecule docked in pocket on FAK is shown on left. INT2-31 is modeled in the pocket on FAK (aa 127-243) corresponding to the site of FAK interaction with IGF-1R.

- **NSC 344553**
- Molecular Weight: 377.31 [g/mol]

- Molecular Formula: $C_{12}H_{16}N_3O_7PS$
- XLogP -1.3
- H-Bond Donor 4
- H-Bond Acceptor 10

- For FAK-NT2
- **Predicted Score:** -50.12093353
- **VDW:** -16.27830696
- **ES:** -33.84262848

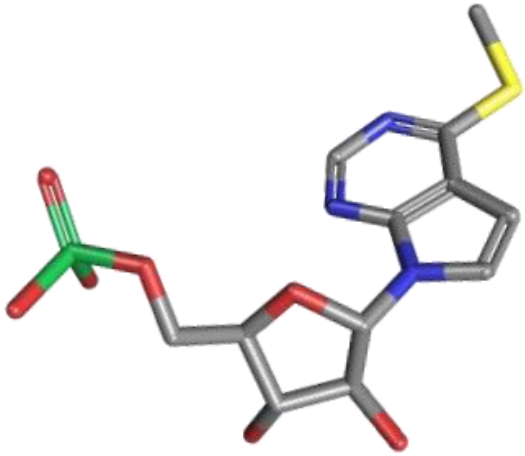

Figure 3-4. The structure of INT2-31 (NSC 344553). Structure and molecular formula of INT2-31 are demonstrated. The energies of interaction between FAK and NSC 344553 are computed as the sum of the van der waals and electrostatic interactions.

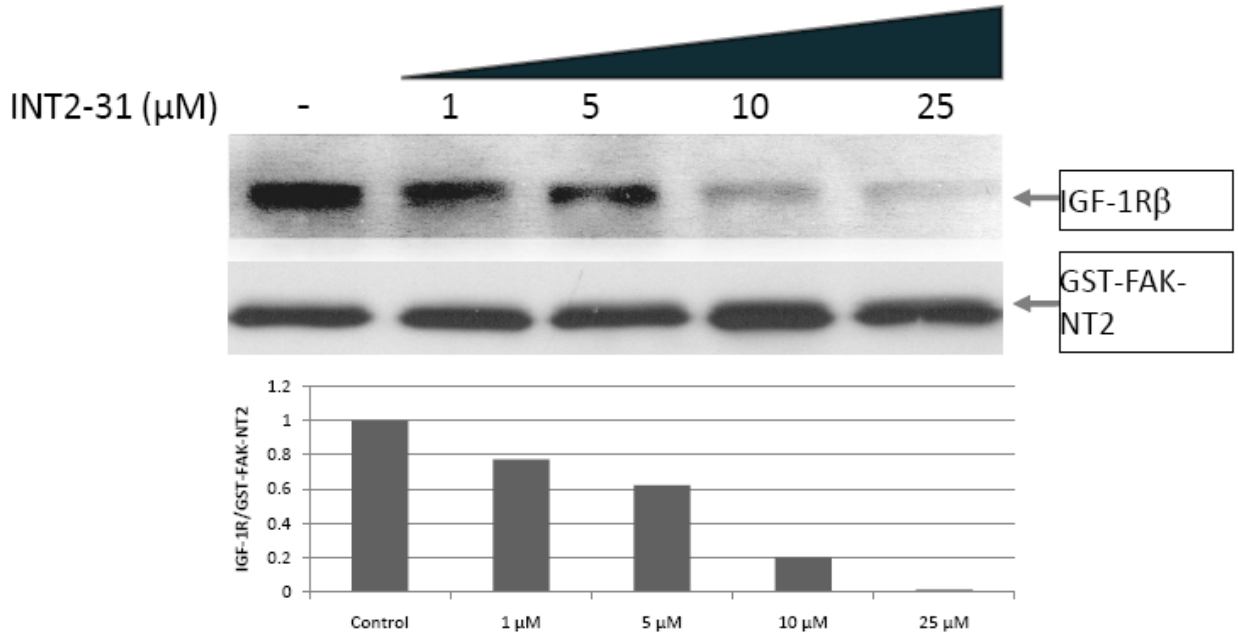

Figure 3-5. GST-FAK-NT2 pull down of IGF-1R□. With increasing doses of INT2-31, 200ng GST-FAK-NT2 pull down of IGF-1R□ is diminished. Densitometry showing ratio of IGF-1R to GST-FAK is shown below Western blot. Average IC_{50} of INT2-31 for disruption of proteins is 3.96 μM.

A

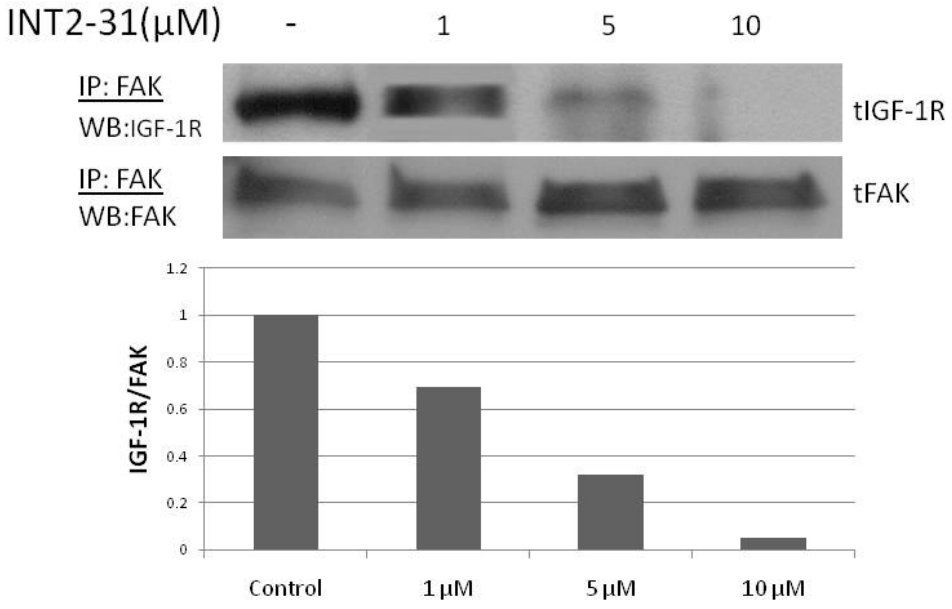

B

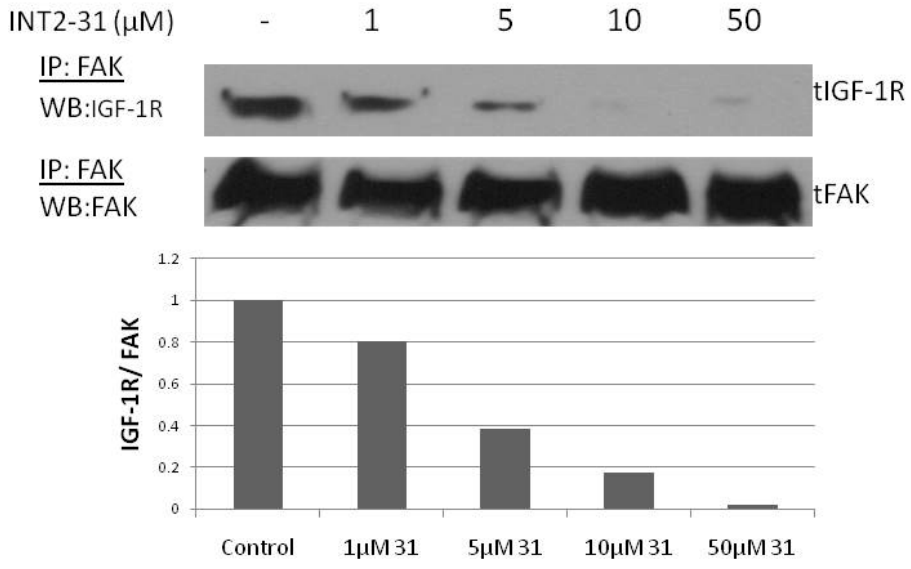

Figure 3-6. Effects of INT2-31 on FAK and IGF-1R interaction. A)With increasing doses of INT2-31, coimmunoprecipitation of FAK and IGF-1R is decreased in C8161 melanoma cells. Densitometry showing the ratio of IGF-1R to FAK is shown below the western blot (IC_{50} = 2.72 μM). B) With increasing doses of INT2-31, coimmunoprecipitation of FAK and IGF-1R is decreased in A375 melanoma cells. Densitometry showing the ratio of IGF-1R to FAK is shown below the western blot (IC_{50} = 3.17 μM).

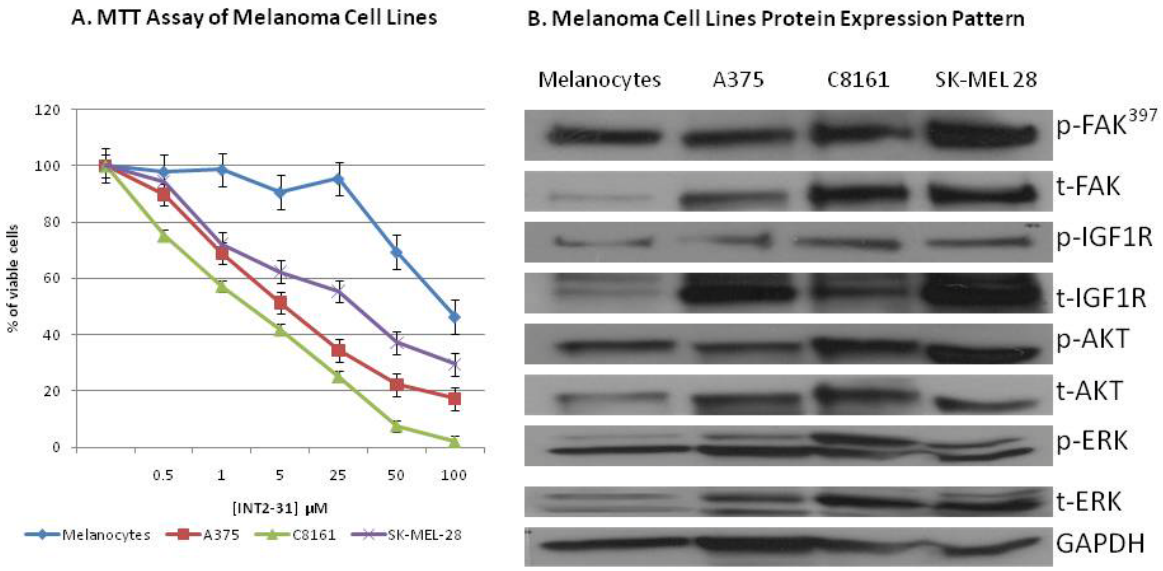

Figure 3-7. Effect of INT2-31 on cell viability. A) MTT Assay of melanoma cell lines showing that INT2-31inhibited the cell viability of normal melanocytes and three melanoma cell lines in a dose dependent fashion over 72 hours, B) Protein expression of FAK, IGF-1R, Akt and ERK in the three melanoma cell lines and melanocytes.

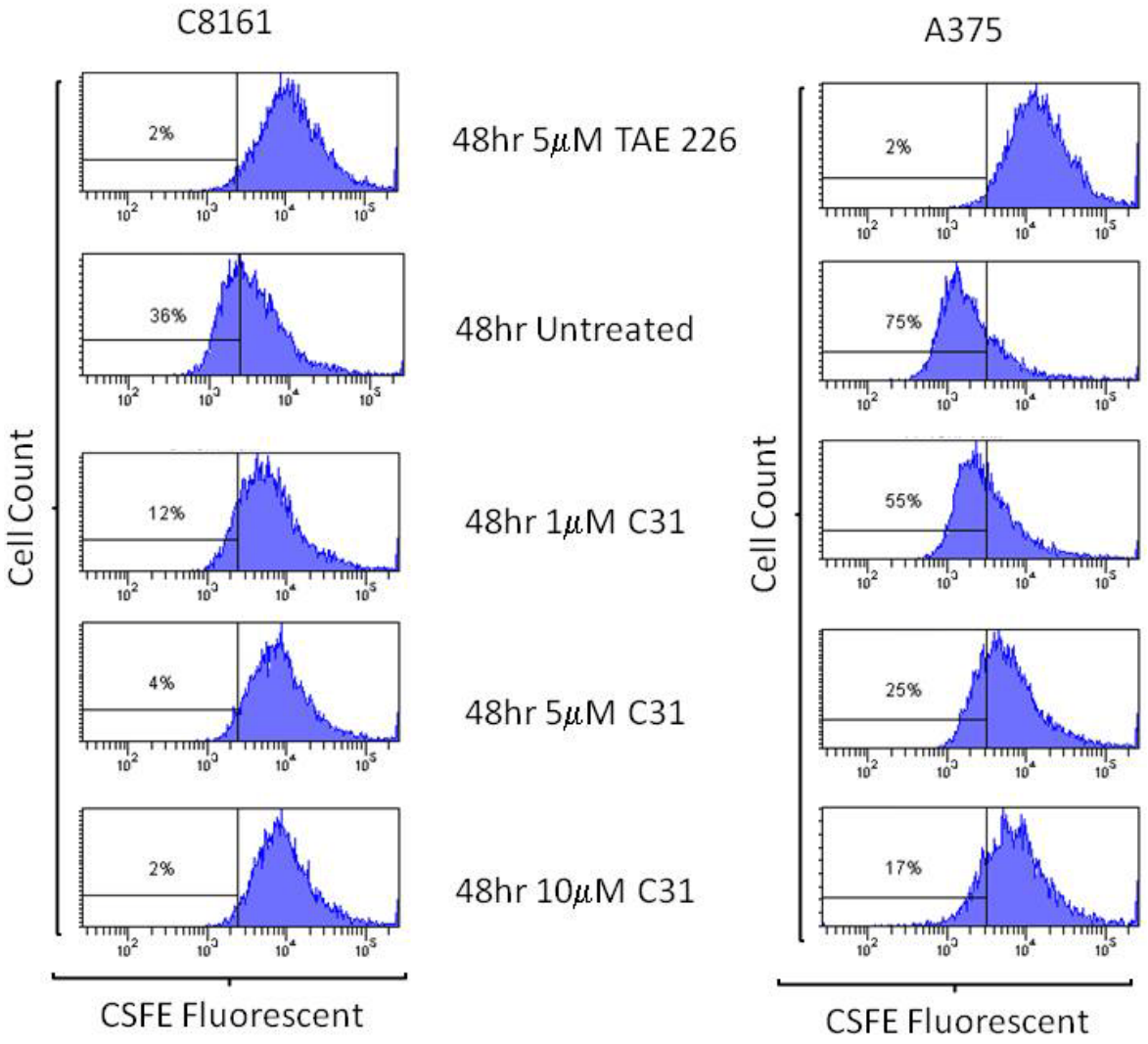

Figure 3-8. CSFE cell proliferation assay with A375 melanoma cells (left) and C8161 melanoma cells (right) in the presence of increasing doses of INT2-31 or TAE 226 (dual FAK and IGF-1R kinase inhibitor).

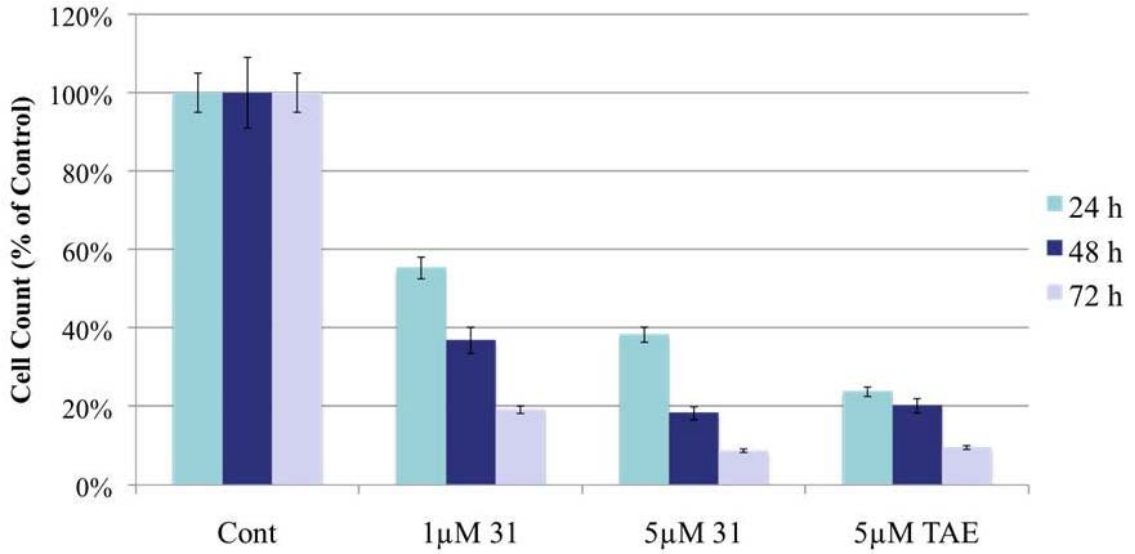

Figure 3-9. C8161 melanoma cell counts in the presence of INT2-31 or TAE 226. There is a dose and time dependent effect with inhibition of cell growth with our lead compound.

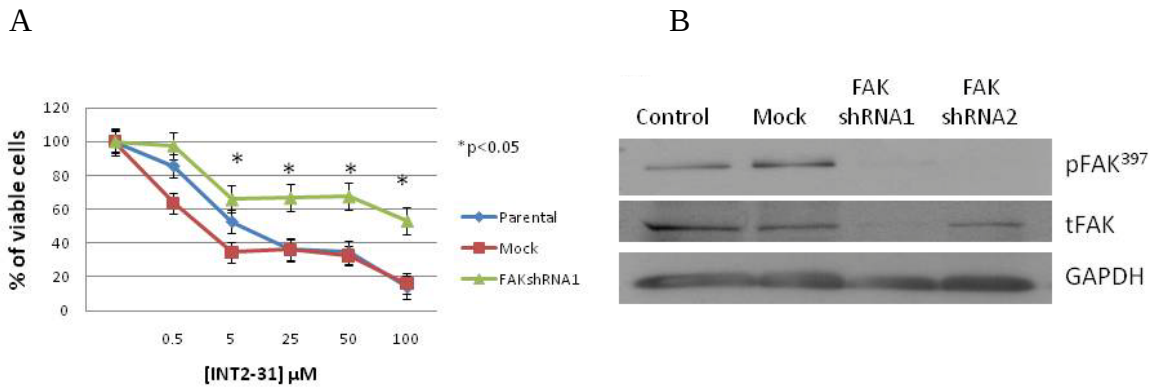

Figure 3-10. Effects of INT2-31 on FAK shRNA transfected C8161 cells. A) MTT assay showing decreased effect of a 72 hour treatment with INT2-31 in C8161 cells expressing FAK shRNA compared to parental and mock transfected cells. B) Western blot showing knockdown of FAK with FAK shRNA. FAK shRNA1 utilized for MTT assay due to greater knockdown of FAK compared to FAK shRNA2.

A

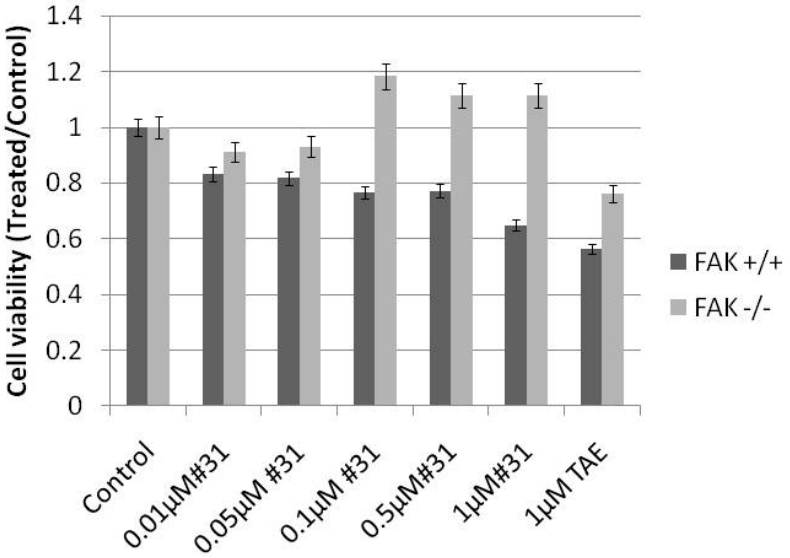

B

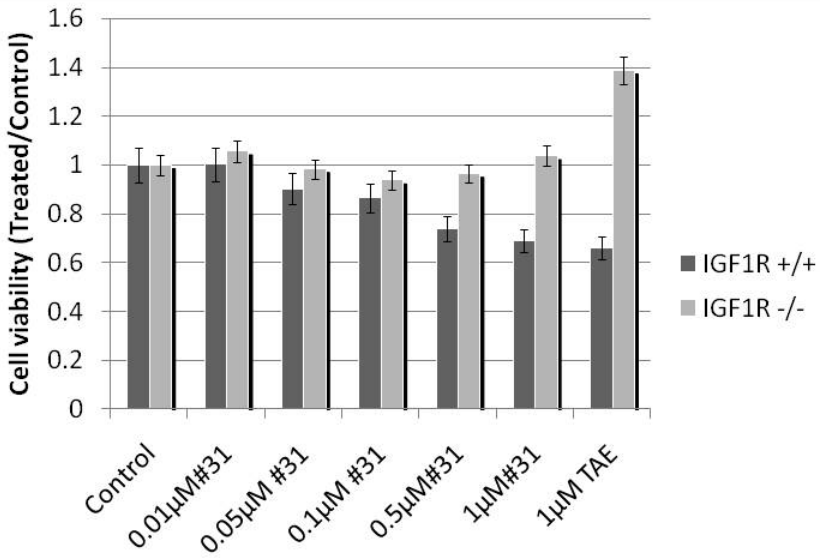

Figure 3-11. Effects of INT2-31 on FAK and IGF-1R deficient MEFs. A) FAK specificity. MTT assay showing the increased effect of INT2-31 (31) or TAE 226 (dual FAK and IGF-1R kinase inhibitor), on FAK wild type fibroblasts compared to null cells. B) IGF-1R specificity. MTT assay showing the increased effect of INT2-31 (31) or TAE 226 (dual FAK and IGF-1R kinase inhibitor), on IGF-1R wild type fibroblasts compared to IGF-1R null cells.

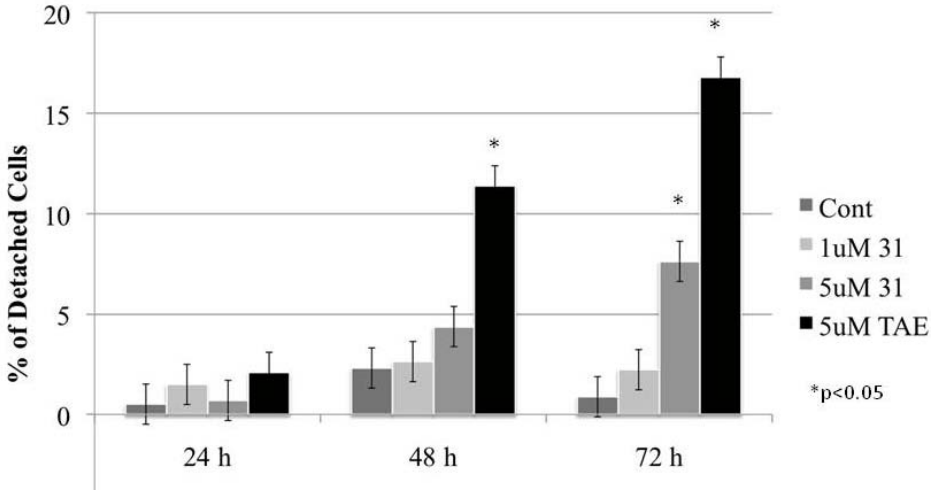

Figure 3-12. Effects of INT2-31 on detachment of C8161 cells. Following treatment with increasing concentrations of INT2-31 or TAE, the number of detached and adherent cells, were counted in three separate experiments, and the average counted numbers used for the graph. There is a dose and time dependent effect on detachment in cells treated with 5 μM INT2-31 at 72 hours. Greater effects are observed with TAE (TAE 226) at 48 and 72 hours (*p<0.05 vs control).

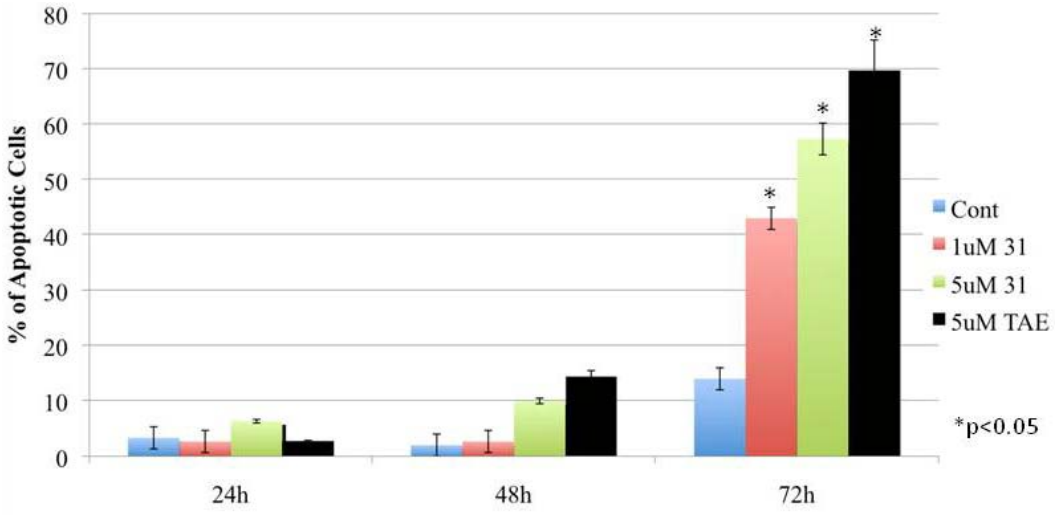

Figure 3-13. Hoescht staining of INT2-31 treated cells. C8161 cells were treated with increasing concentrations of INT2-31 or TAE 226 for 24, 48 and 72 hours, and stained with Hoechst 33342 by adding 1 μg/ml to the fixed cells and 10 μl of cells were mounted on glass coverslips. The slides were viewed under a Zeiss microscope for apoptotic nuclei. The percent of apoptotic cells was calculated as the ratio of apoptotic cells to total number of cells. Over 300 cells per sample were analyzed in three separate experiments, and the average counted numbers used for the graph.

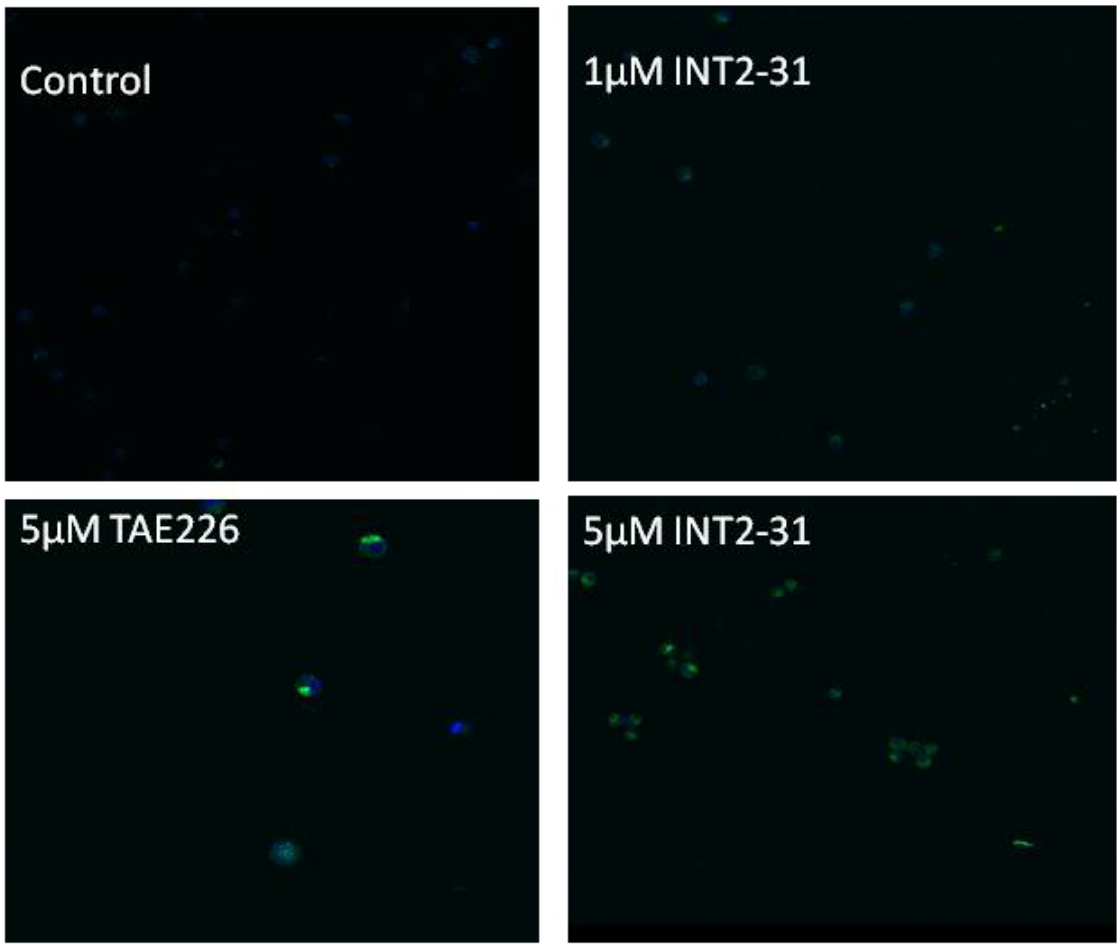

Figure 3-14. Confocal image of Caspase 3/7 activated INT2-31 treated cells. In a 96-well glass bottom plate, 2000 C8161 cells were plated and treated with 5 □M INT2-31 or TAE 226 for 48 hours. Activation of Caspase 3/7 was detected by adding 10 µl of profluorescent caspase-3/7 consensus substrate to 100µl medium and incubated for 30 minutes in the dark at room temperature. Activation of caspase-3/7 enzymes was detected by imaging with a Leica TCS SP5 laser-scanning confocal microscope, when excited at a wavelength of 498nm and emission of 521nm and representative images were captured.

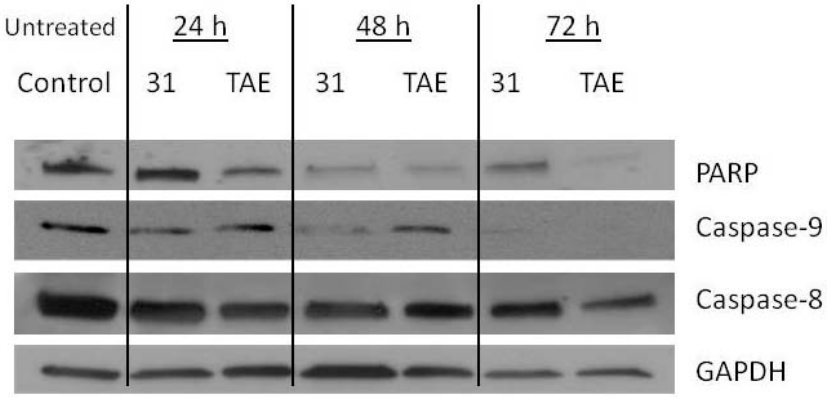

Figure 3-15. Western blot analysis of biochemical markers of the apoptotic pathway. C8161 cells were plated into a 6-well plate and treated with 5 □M INT2-31 or TAE 226 for 24, 48, and 72 hours. Subsequently, cells were lysed and used for western blot analysis.

A

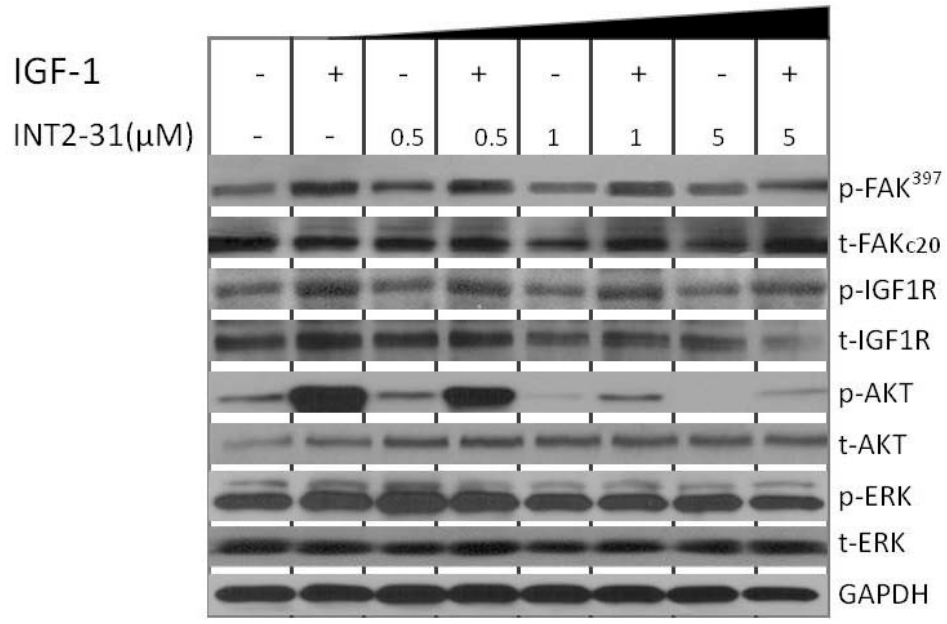

B

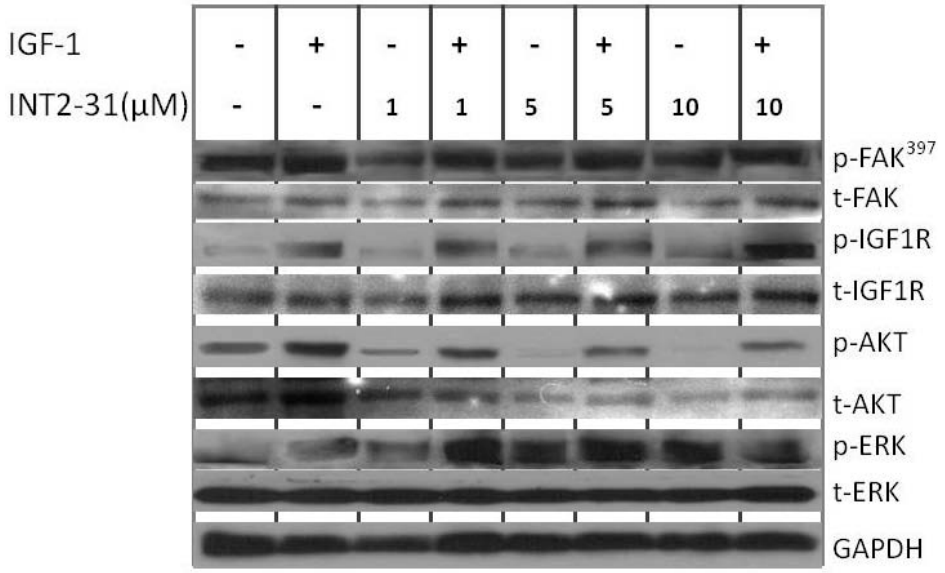
IGF-1
INT2-31(μM)
- + - + - + - +
- - 1 1 5 5 10 10
p-FAK397
t-FAK
p-IGF1R
t-IGF1R
p-AKT
t-AKT
p-ERK
t-ERK
GAPDH

C

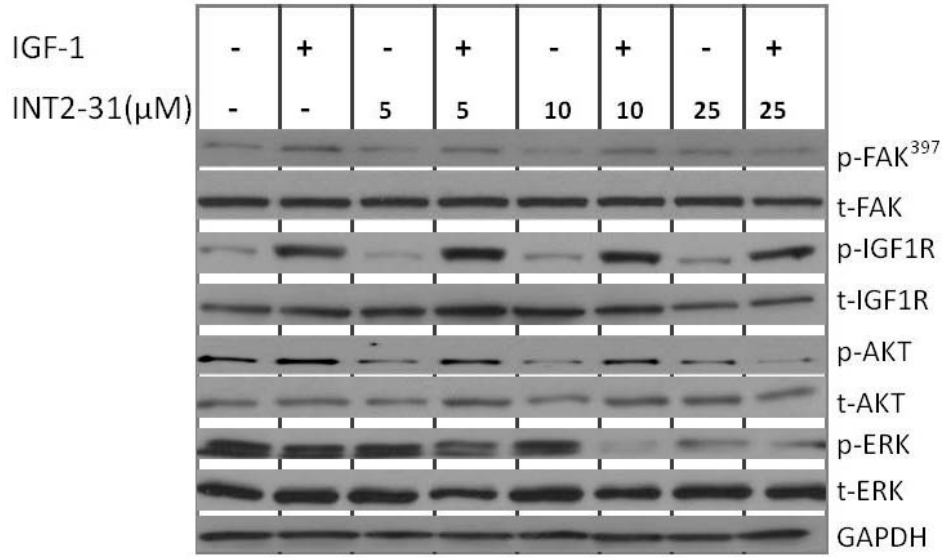
IGF-1
INT2-31(μM)
- + - + - + - +
- - 5 5 10 10 25 25
p-FAK397
t-FAK
p-IGF1R
t-IGF1R
p-AKT
t-AKT
p-ERK
t-ERK
GAPDH

D

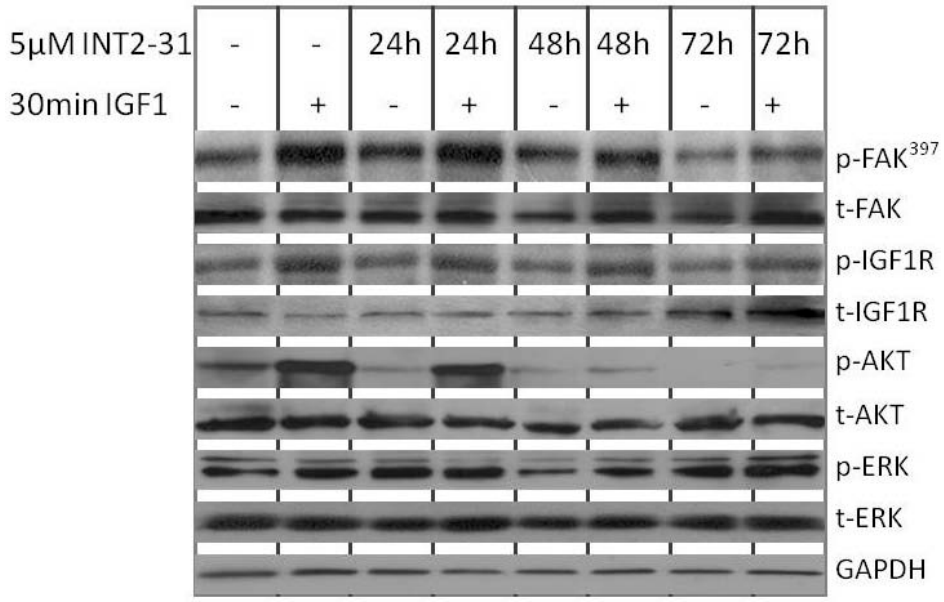

Figure 3-16. Western blot analysis of phosphorylated and total proteins from INT2-31 treated cells. A) C8161 cells were plated into a 6-well plate and treated with increasing concentrations of INT2-31 for 24 hours. B) A375 cells were plated into a 6-well plate and treated with increasing concentrations of INT2-31 for 24 hours. C) SK-MEL-28 cells were plated into a 6-well plate and treated with increasing concentrations of INT2-31 for 24 hours D) C8161 cells were plated into a 6-well plate and treated with 5 μM INT2-31 for 24, 48, and 72 hours.

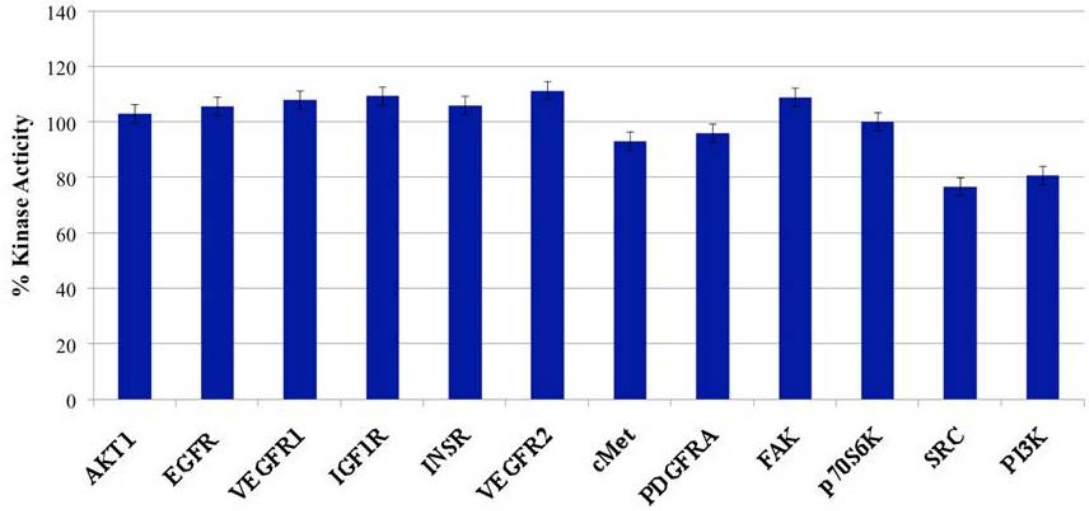

Figure 3-17. Effects of INT2-31 on *in vitro* kinase activity. 1 μM of INT2-31 did not significantly inhibit the kinase activity of these 12 kinases. The maximal inhibition of kinase activity was 22%.

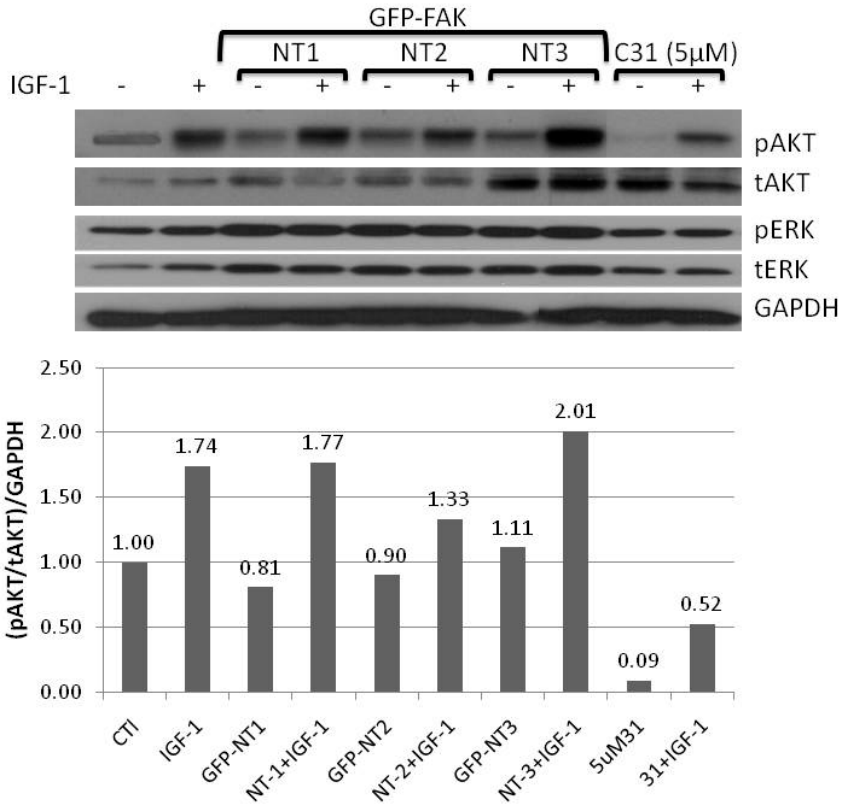

Figure 3-18. Overexpression of FAK-NT2 fragment reduces IGF-1 induced phosphorylation of AKT. C8161 cells transfected with 3 GFP fragments of the FAK N-terminus (FAK NT1, FAK NT2 and FAK NT3).

A

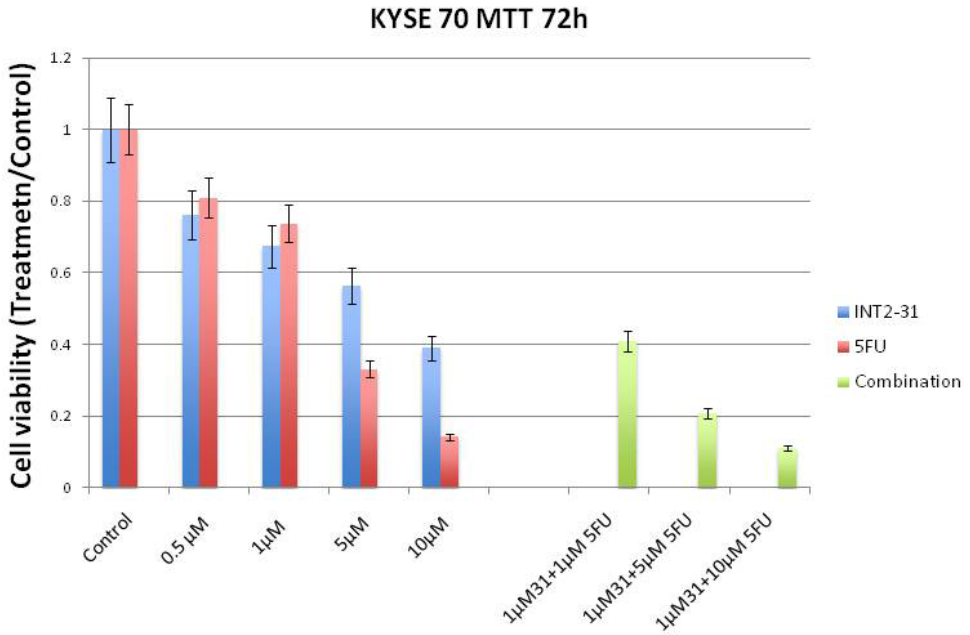

B

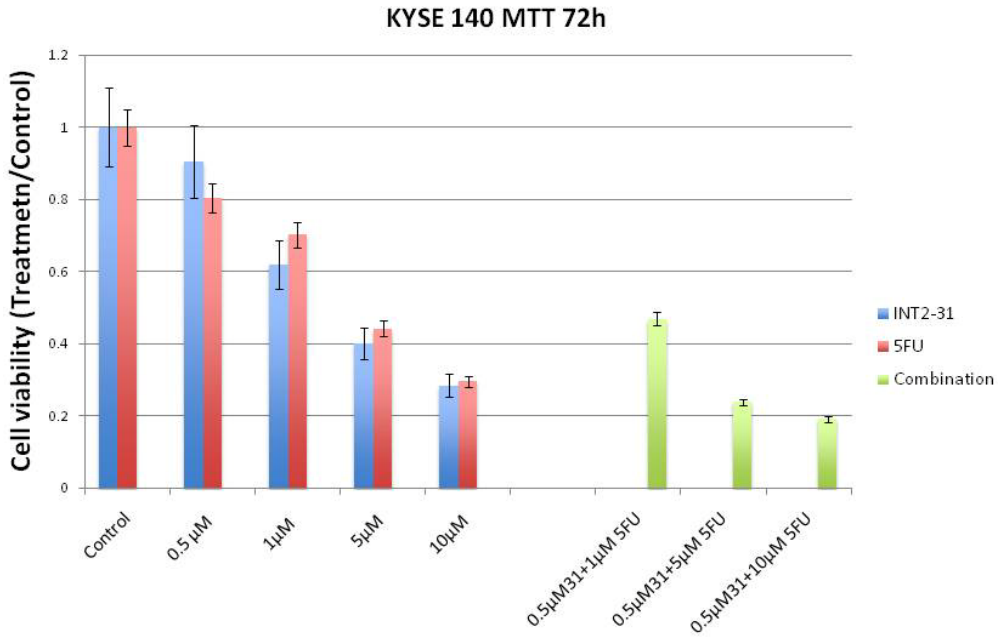

Figure 3-19. INT2-31 sentisized esophageal cancer cells to chemotherapy. MTT assay showing the viability of A) KYSE70 and B) KYSE140 esophageal cancer cell lines treated with increasing concentrations of INT2-31, 5-FU or combination for 72 hours.

A

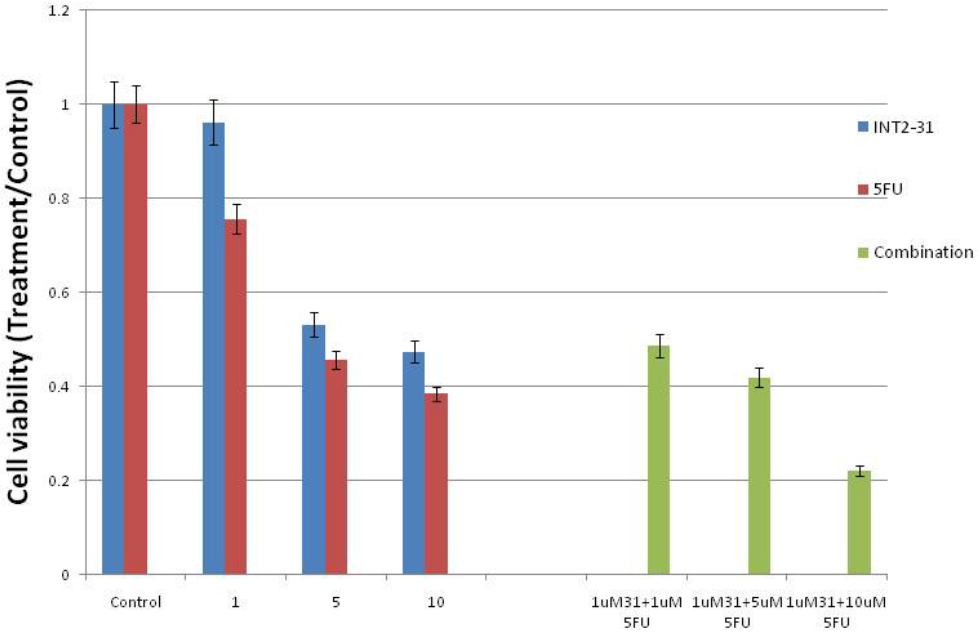

Figure 3-20. INT2-31 sentisized pancreatic cancer cells to chemotherapy. A)MTT assay showing the viability of Panc-1 cell lines treated with increasing concentrations of INT2-31, 5-FU or combination for 72 hours.

A

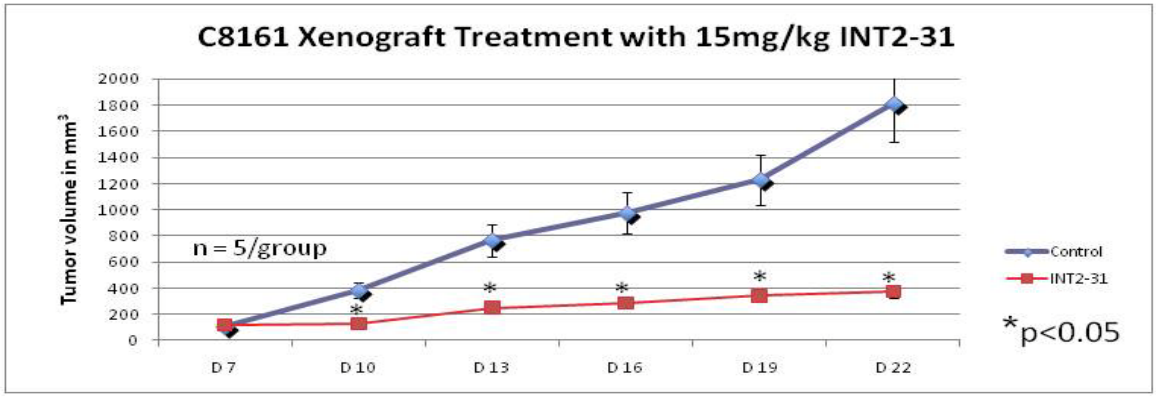
C8161 Xenograft Treatment with 15mg/kg INT2-31
Tumor volume in mm³
2000
1800
1600
1400
1200
1000
800
600
400
200
0
n = 5/group
D 7
D 10
D 13
D 16
D 19
D 22
Control
INT2-31
*p<0.05

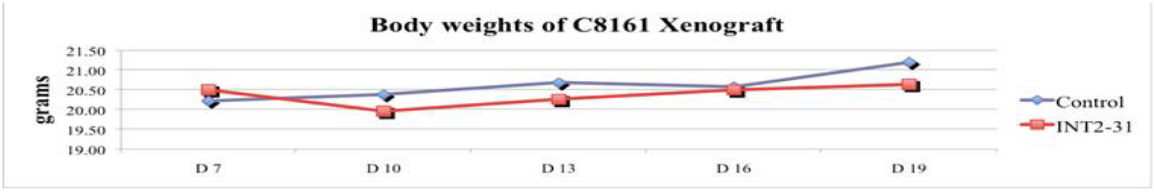
Body weights of C8161 Xenograft
grams
21.50
21.00
20.50
20.00
19.50
19.00
D 7
D 10
D 13
D 16
D 19
Control
INT2-31

B

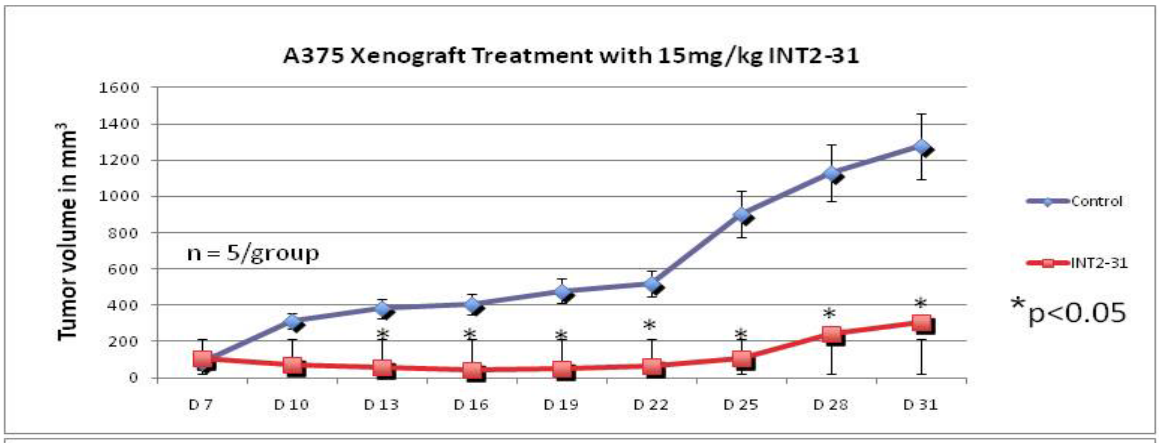
A375 Xenograft Treatment with 15mg/kg INT2-31
Tumor volume in mm³
1600
1400
1200
1000
800
600
400
200
0
n = 5/group
D 7
D 10
D 13
D 16
D 19
D 22
D 25
D 28
D 31
Control
INT2-31
*p<0.05

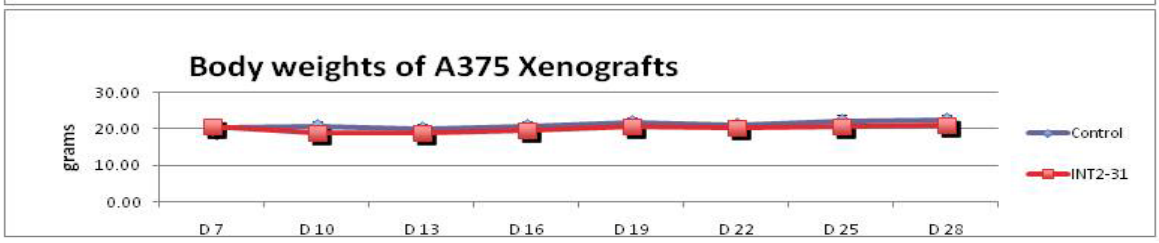
Body weights of A375 Xenografts
grams
30.00
20.00
10.00
0.00
D 7
D 10
D 13
D 16
D 19
D 22
D 25
D 28
Control
INT2-31

C

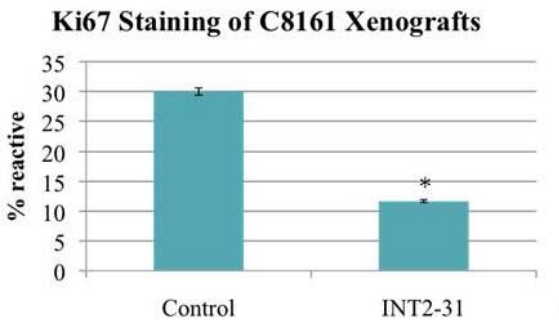

*p<0.05

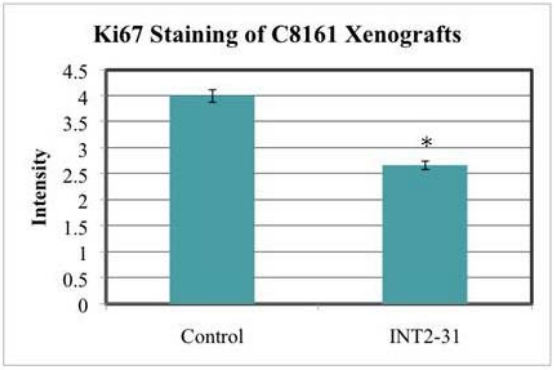

Control

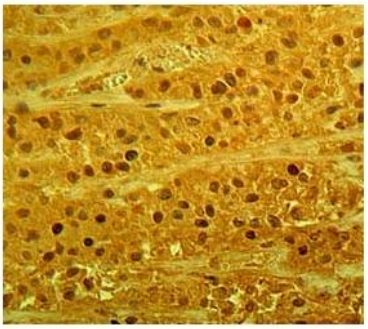

INT2-31 Treated

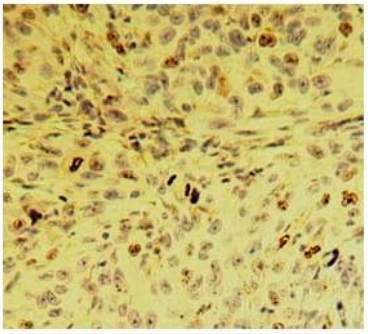

D

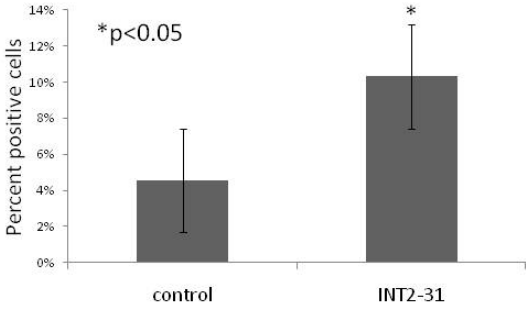

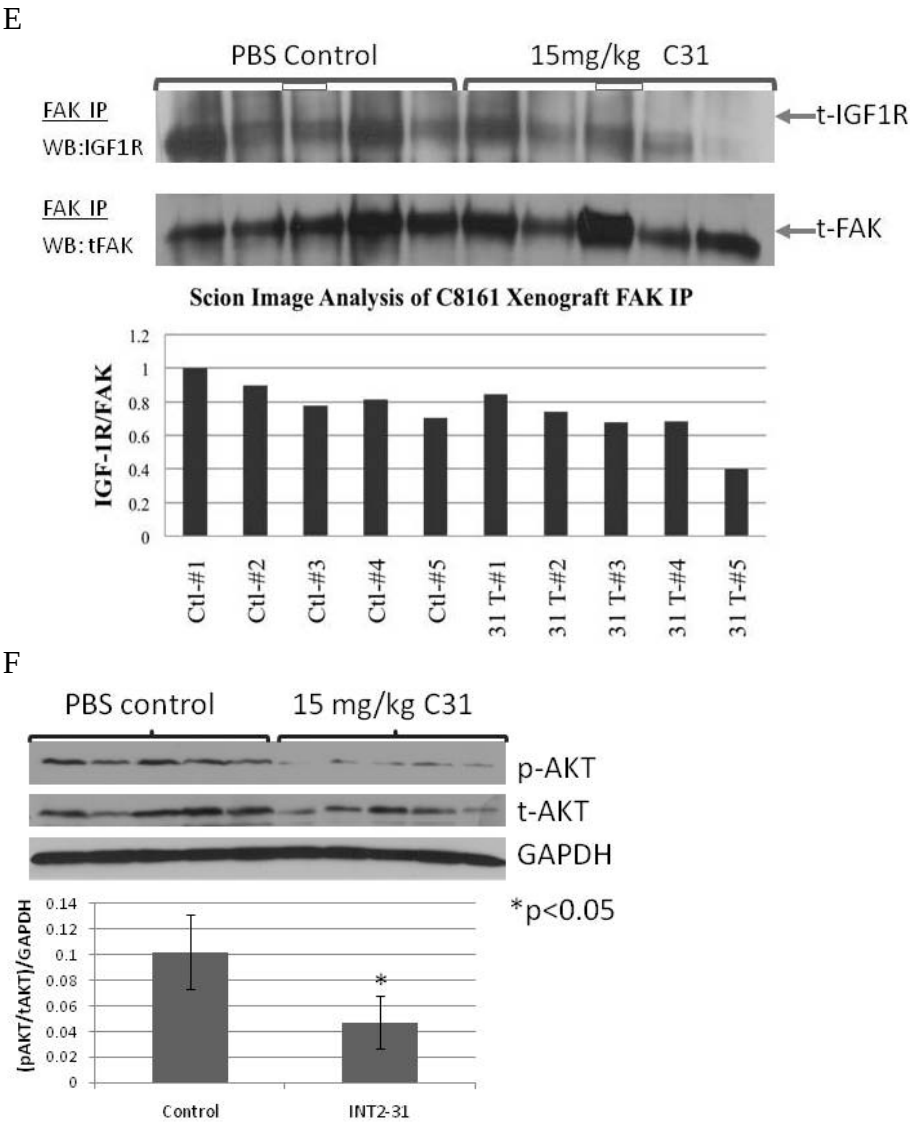

Figure 3-21. Melanoma xenograft analysis. A) Animals were inoculated subcutaneously with C8161 or B) A375 tumor cells and were treated with 15 mg/kg of INT2-31 vs PBS via intraperitoneal injection. Treatment was started on day 7 after tumor implantation. Animal weights are shown below growth curves. * $p<0.05$ C) Ki67 staining of C8161 tumors treated with INT2-31, 15 mg/kg, vs PBS control. The percent of reactive cells is shown in the upper graph. The intensity of staining is shown in the lower graph. The representative micrographs on the right demonstrate the staining patterns. * $p<0.05$ D) TUNEL staining of excised tumors at the completion of the experiment. * $p<0.05$ E) The effect of INT2-31 on the coimmunoprecipitation of FAK and IGF-1R from tumor specimens. The lower graph shows the densitometry of the ratio of the IGF-1R to FAK signal. F) The effect of INT2-31 (15 mg/kg) on the phosphorylation of AKT *in vivo*.

A

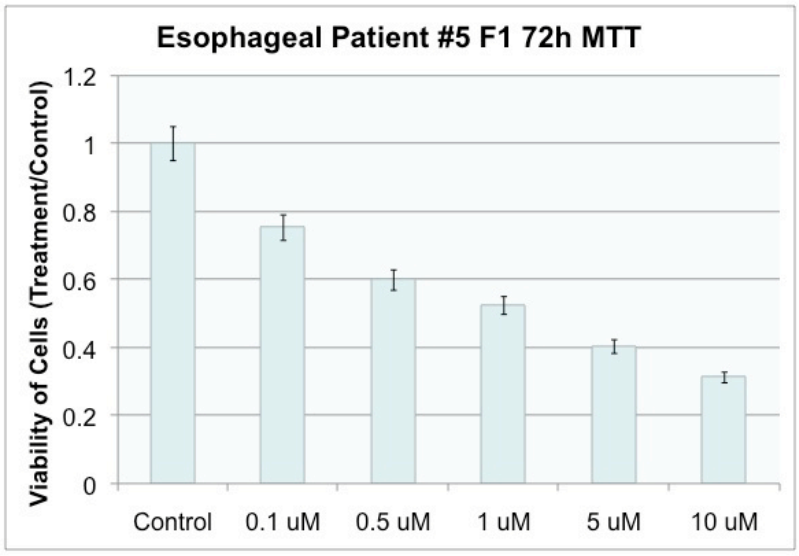
Esophageal Patient #5 F1 72h MTT
Viability of Cells (Treatment/Control)
1.2
1
0.8
0.6
0.4
0.2
0
Control
0.1 uM
0.5 uM
1 uM
5 uM
10 uM

B

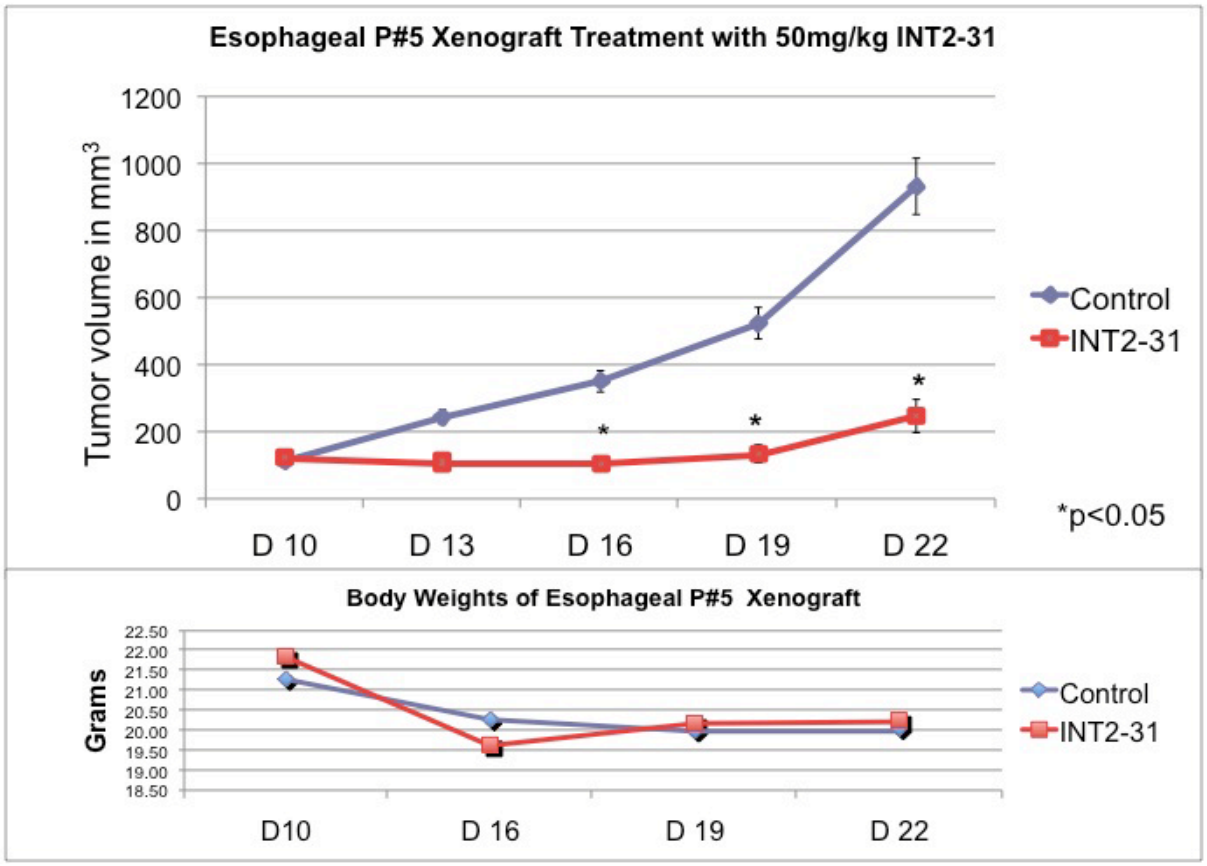
Esophageal P#5 Xenograft Treatment with 50mg/kg INT2-31
Tumor volume in mm3
1200
1000
800
600
400
200
0
D 10
D 13
D 16
D 19
D 22
Control
INT2-31
*p<0.05
Body Weights of Esophageal P#5 Xenograft
Grams
22.50
22.00
21.50
21.00
20.50
20.00
19.50
19.00
18.50
D10
D 16
D 19
D 22
Control
INT2-31

C

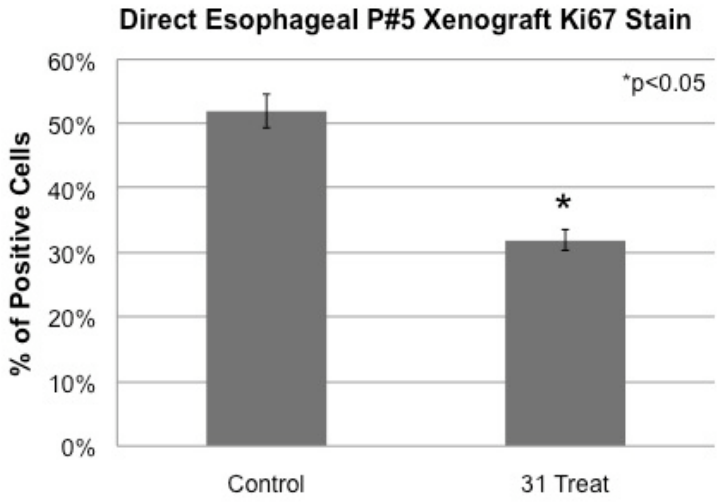

Figure 3-22. Effects of INT2-31 on direct esophageal cancer patient#5 specimen. A) MTT assay showing that increasing concentrations of INT2-31inhibited the cell viability of esophageal patient #5 cells. B) Esophageal patient #5 xenografts were treated with 50 mg/kg of INT2-31 vs PBS via intraperitoneal injection. Treatment was started on day 10 after tumor implantation. Animal weights are shown below growth curves. * $p<0.05$ C) The percentage of reactive cells stained with Ki67 antibody is shown in the treatment vs control xenografts. * $p<0.05$.

A

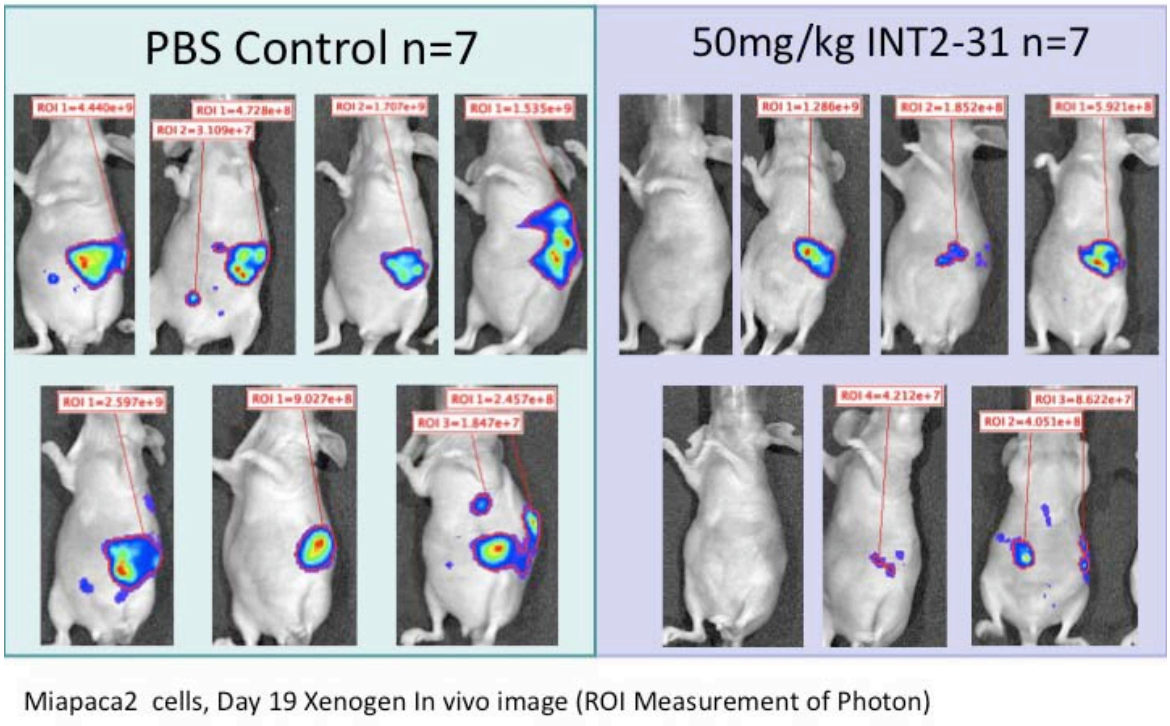

Miapaca2 cells, Day 19 Xenogen In vivo image (ROI Measurement of Photon)

B

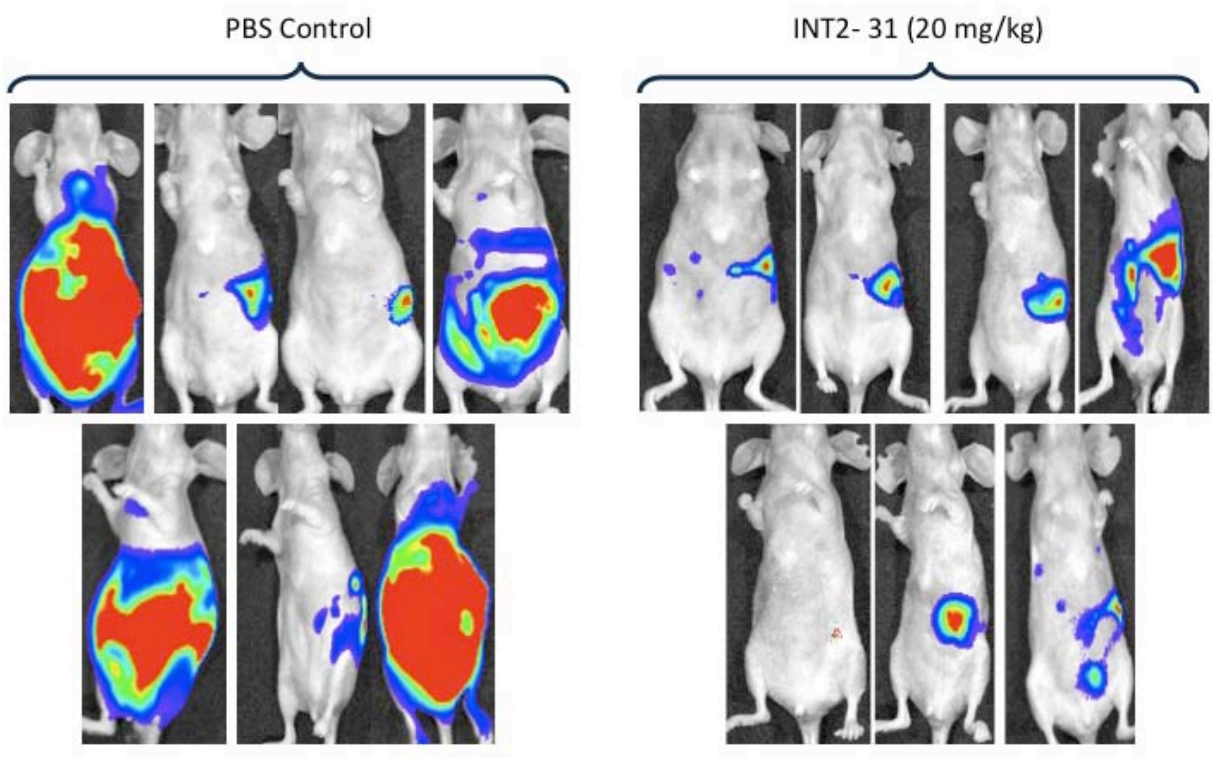

Figure 3-23. Effects of INT2-31 on orthotopic pancreatic mice model. A) Miapaca-2 xenografts were treated with 50 mg/kg of INT2-31 vs PBS via intraperitoneal injection. Treatment was started on day 7 after tumor implantation. B) Panc-1 xenografts were treated with 15 mg/kg of INT2-31 vs PBS via subcutaneous injection. Treatment was started on day 15 after tumor implantation.

LIST OF REFERENCES

Allegra CJ, Grem JL. Antimetabolites. (1997). In: V. T. DeVita, S. Hellman, and S. A. Rosenberg (eds.), Cancer: Principles and Practice of Oncology, Ed. 5, pp. 432–452. Philadelphia: Lippincott-Raven.

Almoguera C, Shibata D, Forrester K, Martin J, Arnheim N, Perucho M. (1988). Most human carcinomas of the exocrine pancreas contain mutant c-K-ras genes. *Cell* **53**: 549-554.

Annabi SE, Gautier N, Baron V. (2001). Focal adhesion kinase and src mediate integrin regulation of insulin receptor phosphorylation. *FEBS Letters* **507**: 247-252.

Arbet-Engels C, Janknecht R, Eckhart W. (1999). Role of focal adhesion kinase in MAP kinase activation by insulin-like growth factor-I or insulin. *FEBS Letters* **454**: 252-256.

Avraham, H, Park SY, Schinkmann K, Avraham S. (2000). RAFTK/Pyk2-mediated cellular signaling. *Cell Signal* **12**: 123–133.

Baron V, Calleja V, Ferrari P, Alengrin F, Van Obberghen E. (1998). p125Fak focal adhesion kinase is a substrate for the insulin and insulin-like growth factor-I tyrosine kinase receptors. *J Biol Chem* **273**: 7162-7168.

Bergmann U, Funatomi H, Kornmann M, Beger HG, Korc M. (1996). Increased expression of insulin receptor substrate-1 in human pancreatic cancer. *Biochem Biophys Res Commun* **220**: 886-890.

Bergmann U, Funatomi H, Yokoyama M, Beger HG, Korc M. (1995). Insulin-like growth factor 1 overexpression in human pancreatic cancer: evidence for autocrine and paracrine roles. *Cancer Res* **55**: 2007-2011.

Blanck HM, Tolbert PE, Hoppin JA. (1999). Patterns of genetic alterations in pancreatic cancer: a pooled analysis. *Environ Mol Mutagen* **33**: 111-122.

Caldas C, Hahn SA, da Costa LT, Redston MS, Schutte M, Seymour AB, Weinstein CL, Hruban RH, Yeo CJ, Kern SE. (1994). Frequent somatic mutations and homozygous deletions of the p16 (MTS1) gene in pancreatic adenocarcinoma. *Nat Genet* **8**: 27-32.

Choi HS, Wang Z, Richmond W, He X, Yang K, Jiang T, Karanewsky D, Gu X J, Zhou V, Liu Y, Che J, Lee C C, Caldwell J, Kanazawa T, Umemura I, Matsuura N, Ohmori O, Honda T, Gray N, He Y. (2006). Design and synthesis of 7H-pyrrolo[2,3-d]pyrimidines as focal adhesion kinase inhibitors. Part 2. *Bioorg Med Chem Lett* **16**: 2689-2692.

Cooper LA, Shen TL, Guan JL. (2003). Regulation of focal adhesion kinase byits amino-terminal domain through an autoinhibitory interaction. *Mol Cell Biol* **23**: 8030-8041.

Corsi JM, Rouer E, Girault JA, Enslen H. (2006). Organization and post-transcriptional processing of focal adhesion kinase gene. *BMC Genomics* **7:** 198.

Dews M, Prisco M, Peruzzi F, Romano G, Morrione A, Baserga B. (2000). Domains of the insulin-like growth factor 1 receptor required for the activation of extracellular signal-regulated kinases. *Endocrinology* **141**: 1289-1300.

Eggermont AM, Testori A, Marsden J, Hersey P, Quirt I, Petrella T, Gogas H, MacKie RM, MacKie RM, Hauschild A. (2009). Utility of adjuvant systemic therapy in melanoma. *Annals of Oncology* **Supplement 6**: 30–34.

Fiedorek FT, Kay ES. (1995). Mapping of the focal adhesion kinase (Fadk) gene to mouse chromosome 15 and human chromosome 8. *Mammalian Genome* **6**: 123-126.

Furukawa T, Chiba R, Kobari M, Matsuno S, Nagura H, Takahashi T. (1994). Varying grades of epithelial atypia in the pancreatic ducts of humans. Classification based on morphometry and multivariate analysis and correlative with positive reactions of carcinoembryonic antigen. *Arch Pathol Lab Med* **118**: 227-234.

Golubovskaya V, Kaur A, Cance W. (2004). Cloning and characterization of the promoter region of human focal adhesion kinase gene: nuclear factor kappa B and p53 binding sites*1. Biochimica et Biophysica Acta (BBA) - *Gene Structure and Expression* **1678**: 111-125.

Golubovskaya VM, Nyberg C, Zheng M, Kweh F, Magis A, Ostrov D, Cance WG. (2008). A Small Molecule Inhibitor, 1,2,4,5-Benzenetetraamine Tetrahydrochloride, Targeting the Y397 Site of Focal Adhesion Kinase Decreases Tumor Growth. *J Med Chem* **51**: 7405-7416.

Golubovskaya VM, Virnig C, Cance WG. (2008). TAE226-induced apoptosis in breast cancer cells with overexpressed Src or EGFR. *Mol Carcinog* **47**: 222-234.

Halder J, Lin YG, Merritt WM, Spannuth WA, Nick AM, Honda T, Kamat AA, Han LY, Kim TJ, Lu C, Tari AM, Bornmann W, Fernandez A, Lopez-Berestein G, Sood AK. (2007). Therapeutic efficacy of a novel focal adhesion kinase inhibitor TAE226 in ovarian carcinoma. *Cancer Res* 15: 10976-10983.

Han EK, McGonigal T, Wang J, Giranda VL, Luo Y. (2004). Functional analysis of focal adhesion kinase (FAK) reduction by small inhibitory RNAs. *Anticancer Res* **24**: 3899–3905.

Hauck CR, Hsia DA, Puente XS, Cheresh DA, Schlaepfer DD. (2002). FRNK blocks v-Src-stimulated invasion and experimental metastases without effects on cell motility or growth. *EMBO J* **21**: 6289–6302.

Hauschild. (2009). Utility of adjuvant systemic therapy in melanoma. *Ann Oncol* **20**:Suppl

Hewish M, Chau I, Cunningham D. (2009). Insulin-like growth factor 1 receptor targeted therapeutics: novel compounds and novel treatment strategies for cancer medicine. *Recent Pat Anticancer Drug Discov* **3**: 54-72.

Hildebrand JD, Taylor JM, Parsons JT. (1996). An SH3 domain-containing GTPase-activating protein for Rho and Cdc42 associates with focal adhesion kinase. *Mol Cell Biol* **16**: 3169-3178.

Hochwald SN, Nyberg C, Zheng M, Zheng D, Wood C, Massoll NA, Magis A, Ostrov D, Cance WG, Golubovskaya V. (2009). A novel small molecule inhibitor of FAK decreases growth of human pancreatic cancer. *Cell Cycle* **8**: 2435-2443.

Huanwen W, Zhiyong L, Xiaohua S, Xinyu R, Kai W, Tonghua L. (2009). Intrinsic chemoresistance to Gemcitabine is associated with constitutive and laminin-induced phosphorylation of FAK in pancreatic cancer cell lines. *Mol Cancer* **8**: 125.

Imsumran A, Adachi Y, Yamamoto H, Li R, Wang Y, Min Y, Piao W, Nosho K, Arimura Y, Shinomura Y, Hosokawa M, Lee CT, Carbone DP, Imai K. (2007). Insulin-like growth factor-I receptor as a marker for prognosis and a therapeutic target in human esophageal squamous cell carcinoma. *Carcinogenesis* **28**: 947-956.

Ishiwata T, Bergmann U, Kornmann M, Lopez M, Beger HG, Korc M. (1997). Altered expression of insulin-like growth factor II receptor in human pancreatic cancer. *Pancreas* **15**: 367-373.

Jaiswal BS, Janakiraman V, Kljavin NM, Eastham-Anderson J, Cupp JE, Liang Y, Davis DP, Hoeflich KP, Seshagiri S. (2009). Combined targeting of BRAF and CRAF or BRAF and PI3K effector pathways is required for efficacy in NRAS mutant tumors. *PLoS One* **4**: e5717.

Jemal A, Murray T, Samuels A, Ghafoor A, Ward E, Thun MJ. (2003). *Cancer statistics, 2003. CA Cancer J Clin* **53**: 5-26.

Jemal A, Tiwari RC, Murray T, Ghafoor A, Samuels A, Ward E, Feuer EJ, Thun MJ. (2004). Cancer Statistics 2004. *CA Cancer J Clin* **54**: 8-30.

Kahana O, Micksche M, Witz IP, Yron I. (2002). The focal adhesion kinase (P125FAK) is constitutively active in human malignant melanoma *Oncogene* **21**: 3969-3977.

Kalinina T, Bockhorn M, Kaifi JT, Thieltges S, Güngör C, Effenberger KE, Strelow A, Reichelt U, Sauter G, Pantel K, Izbicki JR, Yekebas EF. (2010). Insulin-like growth factor-1 receptor as a novel prognostic marker and its implication as a Co-Target in the treatment of human adenocarcinoma of the esophagus. *Int J Cancer Jan* **26**. [Epub ahead of print]

Kanter-Lewensohn L, Dricu A, Girnita L, Wejde J, Larsson O. (2000). Expression of insulin-like growth factor-1 receptor (IGF-1R) and p27Kip1 in melanocytic tumors: a potential regulatory role of IGF-1 pathway in distribution of p27Kip1 between different cyclins. *Growth Factors* **17**: 193-202.

Kanter-Lewensohn L, Dricu A, Wang M, Wejde J, Kiessling R, Larsson O. (1998). Expression of the insulin-like growth factor-1 receptor and its anti-apoptotic effect in malignant melanoma: a potential therapeutic target. *Melanoma Res* **8**: 389-397.

Kim B, Cheng H-L, Margolis B, Feldman EL. (1998). Insulin receptor substrate 2 and Shc play different roles in insulin-like growth factor 1 signaling. *J Biol Chem* **273**: 34543-34550.

Kloppel G, Bommer G, Ruckert K, Seifert G. (1980). Intraductal proliferation in the pancreas and its relationship to human and experimental carcinogenesis. *Virchows Arch* **387**: 221-233.

Korc M. (1998). Role of polypeptide growth factors and their receptors in human pancreatic cancer. In: Reber HA, ed. Pancreatic Cancer: Pathogenesis, Diagnosis, and Treatment. Totowa, NJ: *Humana Press*: **:**21-29.

Kozuka S, Sassa R, Taki T, Masamoto K, Saga S, Hasegaw K, Takeuchi M. (1979). Relation of pancreatic duct hyperplasia to carcinoma. *Cancer* **43**: 1418-1428.

Lebrun P, Baron V, Hauck CR, Schlaepfer DD, Van Obberghen E. (2000). Cell adhesion and focal adhesion kinase regulate insulin receptor substrate-1 expression. *J Biol Chem* **275** : 38371-38377.

Liu YC, Leu CM, Wong FH, Fong WS, Chen SC, Chang C, Hu CP. (2002). Autocrine stimulation by insulin-like growth factor I is involved in the growth, tumorigenicity and chemoresistance of human esophageal carcinoma cells. *J Biomed Sci* **9**: 665-674.

Liu TJ, LaFortune T, Honda T, Ohmori O, Hatakeyama S, Meyer T, Jackson D, de Groot J, Yung WK. (2007). Inhibition of both focal adhesion kinase and insulin-like growth factor-I receptor kinase suppresses glioma proliferation *in vitro* and *in vivo*. *Mol Cancer Ther* **6**: 1357-1367.

Liu W, Bloom DA, Cance WG, Golubovskaya V, Kurenova E, Hochwald SN. (2008). FAK and IGF-IR interact to provide survival signals in human pancreatic adenocarcinoma cells. *Carcinogenesis* **29**: 1096-107.

Lli cacute D, Furuta Y, Kanazawa S, Takeda N, Sobue K, Nakatsuji N, Nomura S, Fujimoto J, Okada M, Yamamoto T, Aizawa S. (1995). Reduced cell motility and enhanced focal adhesion contact formation in cells from FAK-deficient mice. *Nature* **377**: 539-544.

Mahlamaki EH, Barlund M, Tanner M, Gorunova L, Hoglund M, Karh R, Kallioniemi A. (2002). Frequent amplification of 8q24, 11q, 17q, and 20q-specific genes in pancreatic cancer. *Genes Chromosomes Cancer* **35**: 353-358.

Manning G, Whyte DB, Martinez R, Hunter T, Sudarsanam S. (2002). The protein kinase complement of the human genome. *Science* **298**: 1912-1934.

McLean GW, Carragher NO, Avizienyte E, Evans J, Brunton VG, Frame MC. (2005). The role of focal-adhesion kinase in cancer - a new therapeutic opportunity. *Nat Rev Cancer* **5**: 505-515.

Miyazaki T, Kato H, Nakajima M, Sohda M, Fukai Y, Masuda N, Manda R, Fukuchi M, Tsukada K, Kuwano H. (2003). FAK overexpression is correlated with tumour invasiveness and lymph node metastasis in oesophageal squamous cell carcinoma. *Br J Cancer* **89**: 140-145.

Orr AW, Murphy-Ullrich JE. (2004). Regulation of endothelial cell function BY FAK and PYK2. *Front Biosci* **9**: 1254-1266.

Ouban A, Muraca P, Yeatman T, Coppola D. (2003). Expression and distribution of insulin-like growth factor-1 receptor in human carcinomas. *Hum. Pathol*. **34**:803–808.

Parsons JT, Slack-Davis J, Tilghman R, Roberts WG. (2008). Focal adhesion kinase: targeting adhesion signaling pathways for therapeutic intervention. *Clin Cancer Res* **14**: 627-632.

Piao W, Wang Y, Adachi Y, Yamamoto H, Li R, Imsumran A, Li H, Maehata T, Ii M, Arimura Y, Lee CT, Shinomura Y, Carbone DP, Imai K. (2008). Insulin-like growth factor-I receptor blockade by a specific tyrosine kinase inhibitor for human gastrointestinal carcinomas. *Mol Cancer Ther* **7**: 1483-1493.

Pisani P, Parkin DM, Bray F, Ferlay J. (1999). Estimates of the worldwide mortality from 25 cancers in 1990. *Int J Cancer* **83**: 18-29.

Pollak M. (2008). Insulin and insulin-like growth factor signaling in neoplasia. *Nat Rev Cancer* **8**: 915-928.

Pour PM, Sayed S, Sayed G. (1982). Hyperplastic, preneoplastic and neoplastic lesions found in 83 human pancreases. *Am J Clin Pathol* **77**: 137-152.

Roberts WG, Ung E, Whalen P, Cooper B, Hulford C, Autry C, Richter D, Emerson E, Lin J, Kath J, Coleman K, Yao L, Martinez-Alsina L, Lorenzen M, Berliner M, Luzzio M, Patel N, Schmitt E, LaGreca S, Jani J, Wessel M, Marr E, Griffor M, Vajdos F. (2008). Antitumor activity and pharmacology of a selective focal adhesion kinase inhibitor, PF-562,271. *Cancer Res* **68**: 1935-1944.

Ruggeri BA, Huang L, Wood M, Cheng JQ, Testa JR. (1998). Amplification and overexpression of the AKT2 oncogene in a subset of human pancreatic ductal adenocarcinomas. *Mol Carcinog* **21**: 81-86.

Shi Q, Hjelmeland AB, Keir ST, Song L, Wickman S, Jackson D, Ohmori O, Bigner DD, Friedman HS, Rich JN. (2007). A novel low-molecular weight inhibitor of focal adhesion kinase, TAE226, inhibits glioma growth. *Mol Carcinog* **46**: 488-496.

Siu LL, Burris HA, Mileshkin L, Camidge DR, Rischin D, Chen EX, Jones S, Yin D, Fingert H. (2007). *Journal of Clinical Oncology, 2007 ASCO Annual Meeting Proceedings Part 1.* **25**: 3527.

Slack-Davis JK, Martin KH, Tilghman RW, Iwanicki M, Ung EJ, Autry C, Luzzio MJ, Cooper B, Kath JC, Roberts WG, Parsons JT. (2007). Cellular characterization of a novel focal adhesion kinase inhibitor. *J Biol Chem* **282**: 14845-14852.

Staal SP. (1987). Molecular cloning of the Akt oncogene and its human homologues AKT1 and AKT2: amplification of AKT1 in a primary human gastric adenocarcinoma. *Proc Natl Acad Sci* **84**: 5034-5037.

Stoeltzing O, Liu W, Reinmuth N, Fan F, Parikh AA, Bucana CD, Evans DB, Semenza GL, Ellis LM. (2003). Regulation of Hypoxia-inducible factor-1alpha, vascular endothelial growth factor, and angiogenesis by an insulin-like growth factor-1 receptor autocrine loop in human pancreatic cancer. *Am J Pathol* **163**: 1001-1011.

Ucar D, Hochwald S. FAK as a therapeutic target in malignancy. *Recent advances in carcinogenesis*, in press.

Valentinis B, Morrione A, Peruzzi F, Prisco M, Reiss K, Baserga R. (1999). Anti-apoptotic signaling of the IGF-1 receptor in fibroblasts following loss of matrix adhesion. *Oncogene* **18**: 1827-1836.

Van Nimwegen MJ, van de Water B. (2007). Focal adhesion kinase: a potential target in cancer therapy. *Biochem Pharmacol* **73**: 597-609.

Vincent AM, Feldman EL. (2002). Control of cell survival by IGF signaling pathways. *Growth Hormone and IGF Research* **12**: 193-197.

Wang ZG, Fukazawa T, Nishikawa T, Watanabe N, Sakurama K, Motoki T, Takaoka M, Hatakeyama S, Omori O, Ohara T, Tanabe S, Fujiwara Y, Shirakawa Y, Yamatsuji T, Tanaka N, Naomoto Y. (2008). TAE226, a dual inhibitor for FAK and IGF-IR, has inhibitory effects on mTOR signaling in esophageal cancer cells. *Oncol Rep* **20**: 1473-1477.

Watanabe N, Takaoka M, Sakurama K, Tomono Y, Hatakeyama S, Ohmori O, Motoki T, Shirakawa Y, Yamatsuji T, Haisa M, Matsuoka J, Beer DG, Nagatsuka H, Tanaka N,

Naomoto Y. (2008). Dual tyrosine kinase inhibitor for focal adhesion kinase and insulin-like growth factor-1 receptor exhibits anticancer effect in esophageal adenocarcinoma *in vitro* and *in vivo*. *Clin Cancer Res* **14**: 4631-4639.

Weiner TM, Liu ET, Craven RJ, Cance WG. (1993). Expression of focal adhesion kinase gene and invasive cancer. *Lancet* **342**: 1024-1025.

Yamamoto D, Sonoda Y, Hasegawa M, Funakoshi-Tago M, Aizu-Yokota E, Kasahara T. (2003). FAK overexpression upregulates cyclin D3 and enhances cell proliferation via the PKC and PI3-kinase-Akt pathways. *Cellular Signaling* **15**: 575-583.

Yujiri T, Nawata R, Takahashi T. (2002). MEK kinase 1 interacts with focal adhesion kinase and regulates insulin receptor substrate-1 expression. *J Biol Chem* **278**: 3846-3851.

Zheng D, Kurenova E, Ucar D, Magis A, Ostrov D, Golubovskaya V, Cance WG, Hochwald SN. (2009). Targeting of the protein interaction site between FAK and IGF-1R. *Biochem Biophys Res Comm* **388**: 301-305.

BIOGRAPHICAL SKETCH

Deniz A. Ucar was born in Ankara, Turkey. After graduating from Ozel Ari Kolleji High School in Ankara, Turkey, she attended University of Istanbul, where she earned her Doctor of Veterinary Medicine (DVM) degree in 1997. After four years as a volunteer and employment in various animal hospitals, Deniz had her own veterinary practice in Ortakoy, Istanbul. Encouraged by her professors, she left her successful veterinary practice to come to the *U.S.* to do science. She came to the *U.S.* speaking no English. While she was learning English at the English Language Institute, she was awarded a scholarship for tuition and then she finished the premedical program at Santa Fe Community College in one year. In 2005, she became a volunteer in the laboratory of Dr. Lung-Ji Chang to gain some experience while waiting her Master's Program application result. Deniz began with the University of Florida's College of Medicine Master's Program in Fall 2005. After joining the laboratory of Dr. Edward Scott, she began working on different projects and completed her master's program in 2007 with a project on establishing a system for the enrichment of cancer initiating cells. After graduation, she continued on to pursue a doctorate also at the University of Florida's College of Medicine. She received her Ph.D. in 2010 and will apply to medical school.